

Nathan Hugh Barr

March 17, 2019

Abstract

Abstract here

Contents

1	Introduction	3
1.1	Research Question	4
1.2	Structure of this thesis	4
2	Theory	5
2.1	Electromagnetic Radiation	5
2.2	Refractive index	6
2.3	Reflectance and Transmittance	7
2.4	Fresnel equations for the ambient-substrate model	8
2.5	Fresnel equations for the ambient-thin film-substrate model	10
2.6	Fresnel equations for a multilayer model	13
2.7	Fresnel Equation Implementation	15
3	Experimental method	16
3.1	Polymers	16
3.2	Polymers used in Solvent Vapour Annealing	18
3.2.1	Homopolymer Chemistry	18
3.3	Polymer Considerations	18
3.3.1	Relevant values	19
3.3.2	List of polymers used in experiments	19
3.4	Spin Coating thin films	19
3.5	Spectrometer Setup	20
3.6	Reflectance measurements in the NanoCalc spectrometer	21
3.7	Reflectance measurement protocol	23
3.7.1	Without Optics	24
3.7.2	With Optics	24
3.8	Fitting of the reflectance data	25
3.9	Bronkhorst mass flow meters	25
3.10	Solvent Vapour Annealing Process	26

3.10.1 Solvent vapour annealing protocol	27
4 Analysis	29
4.1 Light source fluctuation	29
4.2 Nano-Calc Simulated Reflectance Curves	32
4.3 Solvent vapour annealing ambient study	35
4.4 Polystyrene	38
4.5 Polyisoprene	39
4.6 Polystyrene-b-polyisoprene	43
5 Bibliography	44
A Fresnel functions and Dispersion files	46
A.1 Functions	46
A.2 Dispersion files curves	47
B Scripts	49
B.1 SVA Protocol - slowslow.fps	49
B.2 Light Source fluctuation study	49
B.3 Nano-Calc simulated reflectance curve	50
B.4 Solvent vapour annealing ambient study	54

Chapter 1

Introduction

In December 2017 and May 2018, I was asked to partake in grazing-incidence small-angle scattering(GISAXS) experiments investigating the structure of thin films at The Cornell High Energy Synchrotron Source (CHESS). A thin film is a thin layer on the nanoscale of polymer deposited onto a wafer, in this case a silicon wafer. The experiments were conducted with the aim of understanding the reorganisation of star-block polymers on a silicon wafer when exposed to vapour annealing. GISAXS maps are used to study how the star-block polymers arranged themselves when the polymer film swells. The swelling dilutes the polymer, lowering the glass transition temperature of the polymers, reducing the viscosity and increasing the chain mobility of the polymer. For diblock copolymers, swelling reduces the interfacial tension between the blocks of the diblock copolymer, and between the polymer blocks and the substrate [1]. GISAXS maps gives the researcher a snapshot of the polymers structure at that point in time. The GISAXS maps can be used to calculate the thickness of the polymer, but fitting a model onto the data is non-trivial and post experiment.

This leads to the used of the experimental method called optical spectral reflectance to measure the thickness of a thin film. Using optical spectral reflectance parallel to GISAXS thin films thickness can be monitored in-situ during the solvent vapour annealing(SVA) protocols. The thickness measurements done at CHESS using the optical spectral reflectance were not optimal since the software's thin film model and the reflectance data did not fit well. Since beam time is precious, this problem was to be investigated back at Roskilde University in between beam times.

Optical spectral reflectance is not the only experimental technique available that can measure thin film thickness, there is Atomic force microscopy, Ellipsometry and X-ray reflectometry. Optical spectral reflectance has been chosen to complement GISAXS because it can be used in-situ and in harsh conditions. The size of the

apparatus plays a huge role as the free space in a synchrotron hutch is limited. It is a primitive technique compared to the other techniques that use electromagnetic radiation, and it is important to investigate how far this technique can be pushed.

This thesis has two purposes. The first purpose is to describe the optical spectral reflectance experimental method and how the NanoCalc XR spectrometer and software made by the company Ocean Optics, (<https://oceanoptics.com/>) is used and can the use be optimised for the polymers used in this thesis. This will serve as an introduction to the apparatus and how light reflects and transmits through the thin film. The second purpose is to investigate how the reflectance measurements change during the solvent vapour annealing of homopolymers and diblock copolymers and if it is possible to infer the thickness of the thin films during the solvent vapour annealing.

1.1 Research Question

What are the advantages and limitations when using optical spectral reflectance for determining the thickness of thin polymer films during solvent vapour annealing?

What is the optimal modelling and fitting method for the optical spectral reflectance measurements and thickness determination of the homopolymers, polystyrene and polyisoprene thin films during solvent vapour annealing?

Can the same thickness determination be used on thin films with a horizontal nano scale structure such as the diblock-copolymer Polystyrene-b-Polyisoprene?

1.2 Structure of this thesis

The structure of this thesis is as follows. Chapter 2 will introduce the basic theory of light propagation through a vacuum and through a transparent medium. It will touch on the complex refractive index and the Fresnel equations used to model the reflectance and transmittance of light illuminating the thin films. Chapter 3 will introduce the polymers, creation of the thin films, the Nanocalc spectrometer and how the measurements are taken.

Chapter 2

Theory

The following theory is based on chapter 2 in both [3] and [4]. In this chapter, basic electromagnetic radiation theory, the definition for the complex refractive index and the definition for the reflectance and transmission of light is introduced. The derivation of the Fresnel equations for multilayer thin films ends the theory needed to understand how the reflectance data is modelled in the analysis chapter, chapter 4.

2.1 Electromagnetic Radiation

Electromagnetic radiation can be expressed as a one dimensional sinusoidal wave using either cos or sin:

$$\varphi = A \sin(\omega t - Kx + \delta), \quad (2.1)$$

where A is the wave amplitude, $K = \frac{2\pi}{\lambda}$ is the propagation number and λ is the wave length, angular frequency $\omega = 2\pi\nu$ where ν is the frequency, time t and initial phase δ . From electromagnetic theory, the radiation is composed of an electric field and magnetic field that are both perpendicular to the direction of propagation. Both fields can be expressed as one-dimension complex sinusoidal wave. A complex number can be expressed as $C = a + ib = Re(C) + iIm(C) = r \cos(\theta) + ir \sin(\theta)$. Using Eulers formula $\exp(i\theta) = \cos(\theta) + i \sin(\theta)$, the one dimension sinusoidal wave can be expressed as:

Find
out
last =

$$\varphi = A \cos(\omega t - Kx + \delta) = Re\{A \exp[i(\omega t - Kx + \delta)]\} = A \exp[i(\omega t - Kx + \delta)]. \quad (2.2)$$

The wave travels to the right if the phase is $(\omega t - Kx)$ and to the left if the phase is $(\omega t + Kx)$. Changing the order of the first two terms in the phase does not change

the propagation of the wave, only the initial phase δ . The wave equation in equation 2.1 uses sin in the expression but the complex wave in equation 2.2 uses cos, it is the same representation of the wave just moved 2π in the positive direction. The electric field and magnetic field can be expressed as:

$$E = E_0 \exp[i(\omega t - Kx + \delta)] \quad (2.3)$$

$$B = B_0 \exp[i(\omega t - Kx + \delta)]. \quad (2.4)$$

The relationship between the electric field and magnetic field is given by $E = cB$, and can be derived using the Maxwell-Faraday equation and one dimension wave equations for the electric and magnetic field:

$$\frac{\partial E}{\partial x} = -\frac{\partial B}{\partial t} \quad (2.5)$$

$$E = E_0 \cos(Kx - \omega t) \quad (2.6)$$

$$B = B_0 \cos(Kx - \omega t). \quad (2.7)$$

Using the Maxwell-Faraday equation the following equation can be formed:

$$\frac{\partial E}{\partial x} = -\frac{\partial B}{\partial t} \quad (2.8)$$

$$-KE_0 \sin(Kx - \omega t) = -\omega B_0 \sin(Kx - \omega t) \quad (2.9)$$

$$E_0 = \frac{\omega}{K} B_0 \quad (2.10)$$

$$E_0 = sB_0. \quad (2.11)$$

The constant $\frac{\omega}{K}$ is expressed as the speed s of the light through a medium. In vacuum the speed is equal to the speed of light $s = c$, through a transparent medium the speed is equal to the speed of light divided by the refractive index of the medium $s = \frac{c}{n}$.

2.2 Refractive index

Light travelling from one medium to another will undergo change. The speed of the light and the wavelength will change, but not the frequency. The refractive index is a material constant which describes the change and is greater than or equal to one. The refractive index is defined as:

$$n \equiv \frac{c}{s}, \quad (2.12)$$

where c is the speed of light and s is the speed of light in the medium. The amplitude of the wave will decrease in the medium because the propagations number $K = \frac{2\pi n}{\lambda}$ increases:

$$E = E_0 \exp \left[i(\omega t - \frac{2\pi n}{\lambda} x + \delta) \right]. \quad (2.13)$$

The change is wavelength is $\lambda = \frac{\lambda_0}{n}$, where λ_0 is the wavelength before entering the medium. The medium can also absorb light, a term is added to the refractive index to correct this, and is called the extinction coefficient k . The complex refractive index is given:

$$N = n - ik. \quad (2.14)$$

Placing the complex refractive index into equation 2.13, it can be seen that the waves amplitude will decrease exponentially.

$$E = E_0 \exp \left[i(\omega t - \frac{2\pi N}{\lambda} x + \delta) \right] = E_0 \exp \left(-\frac{2\pi k}{\lambda} x \right) \exp \left[i(\omega t - \frac{2\pi n}{\lambda} x + \delta) \right] \quad (2.15)$$

It needs to be stated that if the phase of the wave is expressed as $(Kx - \omega t)$ and the complex refractive index is given by $N = n - ik$, the exponentially factor will be positive which is incorrect. If the phase of the wave is expressed as $(Kx - \omega t)$ the complex refractive index must be defined as $N = n + ik$.

2.3 Reflectance and Transmittance

When light is reflected upon a surface at an oblique angle, light is reflected and transmitted. The electric field of light is grouped into two oscillation directions which can be defined by two planes, the parallel plane p and the perpendicular plane s. The same applies for the magnetic field of light. The parallel plane is defined by the incident and reflected light and the perpendicular plane is perpendicular to the parallel plane. Theory of light regards the two oscillation directions as the p-polarisation and s-polarisation. The reflectance of both p-polarisation and s-polarisation are defined by the ratio of reflected light intensity by the incident light intensity.

$$R_p \equiv \frac{I_{r,p}}{I_{i,p}} = \frac{|E_{r,p}|^2}{|E_{i,p}|^2} = |r_p|^2 \quad R_s \equiv \frac{I_{r,s}}{I_{i,s}} = \frac{|E_{r,s}|^2}{|E_{i,s}|^2} = |r_s|^2 \quad (2.16)$$

The transmittance can also be expressed using the intensity ratio, $I = N |E|^2$ and the ratio cross-sectional area for the transmitted and incident ray.

$$T_p \equiv \frac{I_{r,p} \cos(\theta_t)}{I_{i,p} \cos(\theta_i)} = \frac{N_t \cos(\theta_t)}{N_i \cos(\theta_i)} \frac{|E_{tp}|^2}{|E_{ip}|^2} = \frac{N_t \cos(\theta_t)}{N_i \cos(\theta_i)} |t_p|^2 \quad (2.17)$$

$$T_s \equiv \frac{I_{r,s} \cos(\theta_t)}{I_{i,s} \cos(\theta_i)} = \frac{N_t \cos(\theta_t)}{N_i \cos(\theta_i)} \frac{|E_{ts}|^2}{|E_{is}|^2} = \frac{N_t \cos(\theta_t)}{N_i \cos(\theta_i)} |t_s|^2 \quad (2.18)$$

$$(2.19)$$

When the extinction coefficient in the refractive index is zero, $k = 0$, the sum of the reflectance and transmittance is equal to one, $R + T = 1$. If the extinction coefficient is greater than zero, $k > 0$, then the sum becomes less than one $R+T < 1$.

2.4 Fresnel equations for the ambient-substrate model

Light is reflected and transmitted at the interface of the ambient and substrate as seen in figure 2.1. The boundary conditions at the interface for the electric and magnetic field in the p-polarisation can be written as:

Need
to
under-
stand
why
B-field
is true

$$E_{i,p} \cos(\theta_i) = E_{t,p} \cos(\theta_t) + E_{r,p} \cos(\theta_r) \quad (2.20)$$

$$\implies E_{t,p} \cos(\theta_t) = E_{i,p} \cos(\theta_i) - E_{r,p} \cos(\theta_r) \quad (2.21)$$

$$B_{i,p} + B_{r,p} = B_{t,p}. \quad (2.22)$$

The subscripts of the electric and magnetic field denote the incident ray i , reflected ray r and transmitted ray t in the p-polarisation p plane. The same boundary conditions for the s-polarisation can be expressed. This introduction to the Fresnel equations will use the p-polarisation light. The boundary conditions of the magnetic field need to be reformulated to express the electric field, this is done using the relation $E = sB$. The magnetic field boundary conditions equation 2.22 can be expressed as:

$$\frac{E_{i,p}}{s_i} + \frac{E_{r,p}}{s_i} = \frac{E_{t,p}}{s_t} \quad (2.23)$$

$$\frac{N_i}{c} (E_{i,p} + E_{r,p}) = \frac{N_t}{c} E_{t,p} \quad (2.24)$$

$$N_i (E_{i,p} + E_{r,p}) = N_t E_{t,p}. \quad (2.25)$$

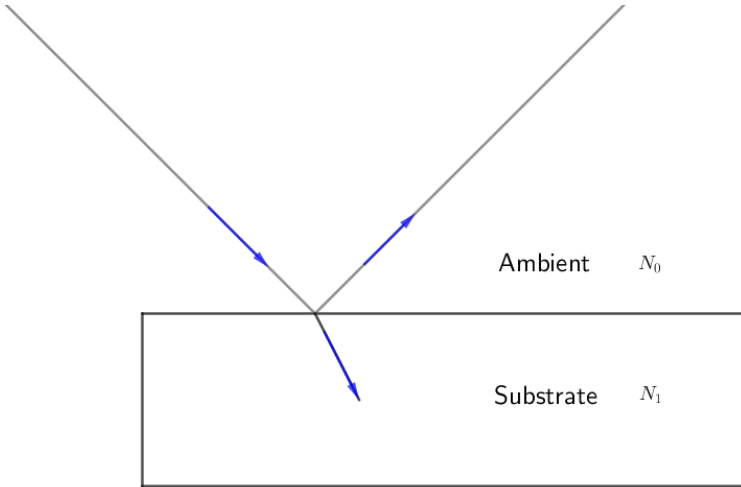


Figure 2.1: The components in this model is an ambient and a substrate both having a refractive index, N_0 and N_1 respectively. Light strikes the substrate reflecting with the same incident angle and refracting into the substrate. Equation 2.31 describes the amplitude reflectance coefficient of a ambient and substrate model.

Though the law of reflection the angle of incident is also the angle of reflection $\theta_i = \theta_r$, placing this into the electric field boundary conditions equation 2.21, the electric field and magnetic field can be expressed as:

$$(E_{i,p} - E_{r,p}) \cos(\theta_i) = E_{t,p} \cos(\theta_t) \quad (2.26)$$

$$\frac{N_i}{N_t} (E_{i,p} + E_{r,p}) = E_{t,p}. \quad (2.27)$$

Placing equation 2.27 into equation 2.26, the amplitude reflectance coefficient and the reflectance can be calculated for the ambient-substrate system:

$$E_{i,p} \cos(\theta_i) - E_{r,p} \cos(\theta_i) = \frac{N_i}{N_t} (E_{i,p} + E_{r,p}) \cos(\theta_t) \quad (2.28)$$

$$E_{i,p} \cos(\theta_i) - \frac{N_i}{N_t} E_{i,p} \cos(\theta_t) = \frac{N_i}{N_t} E_{r,p} \cos(\theta_t) + E_{r,p} \cos(\theta_i) \quad (2.29)$$

$$E_{i,p} (N_t \cos(\theta_i) - N_i \cos(\theta_t)) = E_{r,p} (N_i \cos(\theta_t) + N_t \cos(\theta_i)) \quad (2.30)$$

$$r_p = \frac{E_{r,p}}{E_{i,p}} = \frac{N_t \cos(\theta_i) - N_i \cos(\theta_t)}{N_i \cos(\theta_t) + N_t \cos(\theta_i)} \quad (2.31)$$

$$R_p = |r_p|^2. \quad (2.32)$$

The amplitude transmission coefficient and transmission can be equivalently formulated.

2.5 Fresnel equations for the ambient-thin film-substrate model

The light reflecting and transmitting in this system will interfere both constructive and destructively. To model the optical interference, the Fresnel equation for reflection will be used:

$$r_{jk,p} = \frac{N_k \cos(\theta_j) - N_j \cos(\theta_k)}{N_k \cos(\theta_j) + N_j \cos(\theta_k)} \quad r_{jk,s} = \frac{N_j \cos(\theta_j) - N_k \cos(\theta_k)}{N_j \cos(\theta_j) + N_k \cos(\theta_k)}. \quad (2.33)$$

The subscripts denote the reflection and transmission at definite interface. For example $r_{jk,p} = r_{01,p}$, denotes the reflection at the ambient-thin film interface. In the ambient-thin film-substrate model, light at the ambient-thin film interface will be both reflected and transmitted into the layer. The transmitted ray will then be reflected and transmitted at the thin film-substrate interface. The reflected and transmitted phenomenon will proceed through out the thin film. The change in phase at the interface is given by $\exp(-i\beta)$. Figure 2.2 represents the ambient-thin film-substrate model, this figure will be used to define the phase variation β .

The phase of the reflected ray will vary at the the ambient-thin film interface. This variation can be expressed as $K_0 \bar{AD}$, where $K_0 = \frac{2\pi N_0}{\lambda}$, is the propagation number in air. The phase variation of the transmitted ray is expressed as $K_1(\bar{AB} + \bar{BC})$, where $K_1 = \frac{2\pi N_1}{\lambda}$, is the propagation number in the thin film. The length difference can be denoted as $\bar{AB} + \bar{BC} - \bar{AD}$, thus the phase variation of this length difference is:

$$\alpha = \frac{2\pi N_1}{\lambda}(\bar{AB} + \bar{BC}) - \frac{2\pi N_0}{\lambda}\bar{AD}. \quad (2.34)$$

Using snells law, $\bar{AD} = \bar{AC} \sin(\theta_0)$ and $\bar{AC} = 2d_1 \tan(\theta_1)$ as seen from figure 2.2, this reduces \bar{AD} to:

$$\sin(\theta_0) = \frac{N_1}{N_0} \sin(\theta_1) \quad (2.35)$$

$$\bar{AD} = 2d_1 \frac{\sin(\theta_1)}{\cos(\theta_1)} \sin(\theta_0) \quad (2.36)$$

$$\implies \bar{AD} = 2d_1 \frac{\sin(\theta_1)^2}{\cos(\theta_1)} \frac{N_1}{N_0}. \quad (2.37)$$

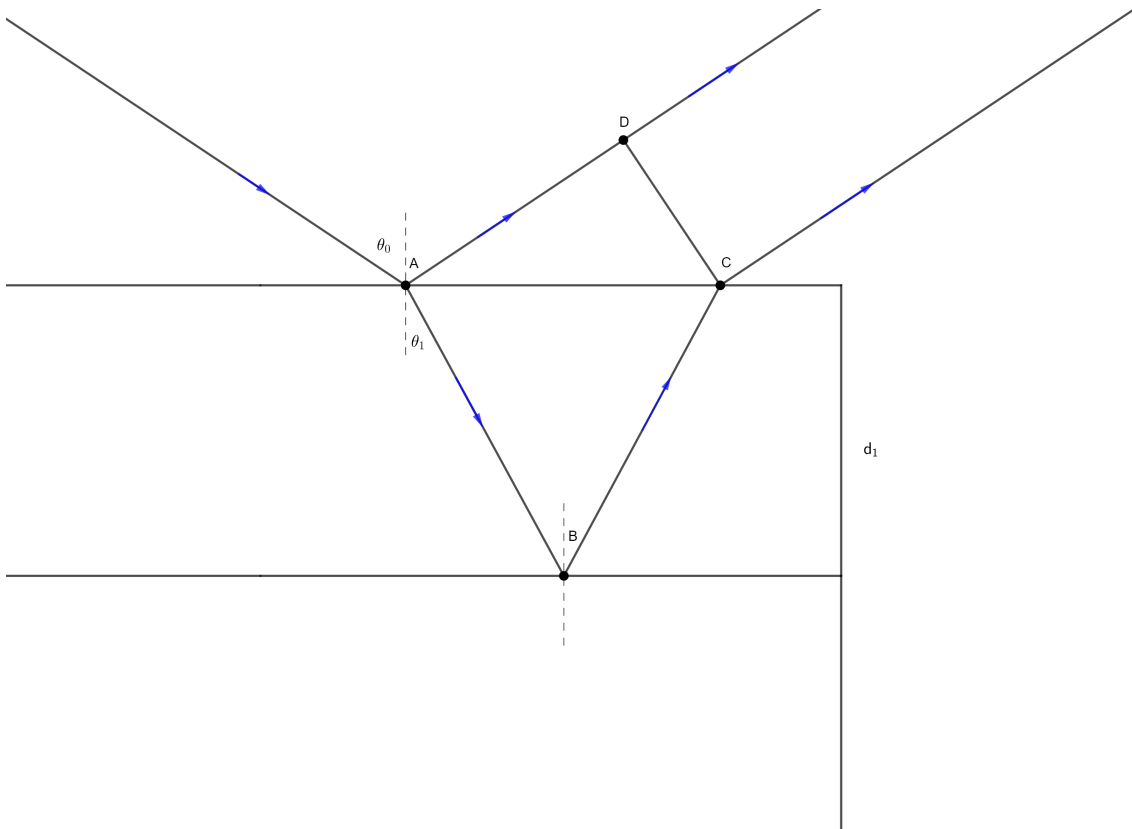


Figure 2.2: Light rays from the left will be reflected and transmitted at point A. The reflected light will experience a phase change at point A. The transmitted light will proceed to point B, where it will reflect undergoing a phase change then transmitting at point C. The phase difference between the primary and secondary ray can be calculated by $\alpha = K_1(\bar{AB} + \bar{BC}) - K_0(\bar{AD})$.

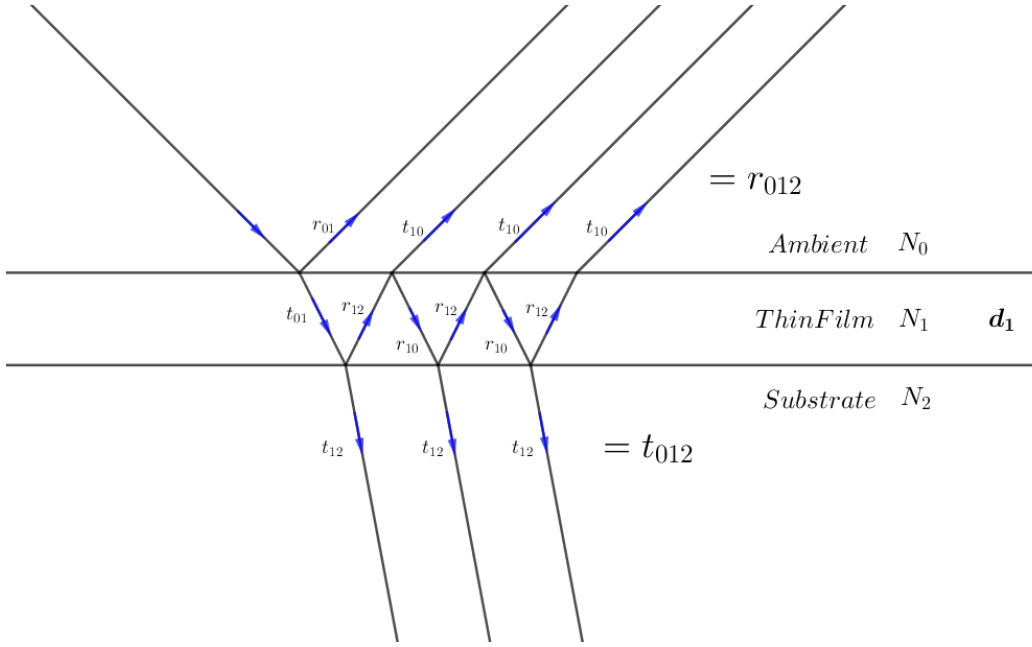


Figure 2.3: When light meets an interface, it reflects or transmits. Each light ray is name either reflection r or transmission t . Each reflected and transmitted ray is also indexed with two numbers, these denote at which interface the light was reflected or transmitted. A variation of phase happens to each reflected and transmitted rays at every interface. The phase variation at an interface can be expressed by the factor $\exp(-i\beta)$. The primary reflected beam is denoted as r_{01} , the second primary reflected beam is denoted $t_{01}r_{12}t_{10}\exp(-i2\beta)$. The reflection amplitude coefficient is the sum of reflected rays that exit the model. The transmission amplitude coefficient is the sum of the transmitted rays that continue into the substrate.

Inserting this into equation 2.34, and $\bar{AB} = \bar{BC} = \frac{d_1}{\cos(\theta_1)}$, as seen from figure 2.2, the equation is reduced to:

$$\alpha = \frac{2\pi N_1}{\lambda} \frac{2d_1}{\cos(\theta_1)} - \frac{2\pi N_0}{\lambda} \frac{2d_1 \sin(\theta_1)^2 N_1}{\cos(\theta_0) N_0} \quad (2.38)$$

$$= \frac{4d_1 \pi N_1}{\lambda} \left(\frac{1 - \sin(\theta_1)^2}{\cos(\theta_1)} \right) \quad (2.39)$$

$$= \frac{4d_1 \pi N_1}{\lambda} \cos(\theta_1). \quad (2.40)$$

α is the total phase difference of the transmitted beam thus the expression $\alpha = 2\beta$ must hold. β is called the film phase thickness and given as:

$$\beta = \frac{2\pi d_1}{\lambda} N_1 \cos(\theta_1). \quad (2.41)$$

Using figure 2.3 as a reference the amplitude reflection coefficient can be ex-

pressed as the sum of the reflected waves. The first time the ray meets the ambient-thin film interface, the ray will reflect and transmit. The reflected ray r_{01} can be calculated using equation 2.31. The transmitted ray will proceed to the next interface reflect back to the ambient-thin film interface and transmit, giving the second reflected wave in the sum expressed as $t_{01}r_{12}t_{10}\exp(-i2\beta)$. The factor $\exp(-i2\beta)$ comes from the phase difference due to the two interactions at the thin film-substrate interface and thin film-ambient interface. The phase difference factor can be collected and multiplied onto the expression since $\varphi = A \exp(i(\omega t - (Kx + 2\beta) + \delta)) = A \exp(i(\omega t - (Kx) + \delta)) \exp(-i2\beta)$. The total amplitude reflection coefficient can be expressed:

$$r_{012} = r_{01} + t_{01}t_{10}r_{12}\exp(-i2\beta) + t_{01}t_{10}r_{10}r_{12}^2\exp(-i4\beta) + t_{01}t_{10}r_{10}^2r_{12}^3\exp(-i6\beta) + \dots \quad (2.42)$$

The amplitude reflection coefficient becomes an infinite geometric series which can be reduced using $y = \frac{a}{(1-r)}$, leading to the coefficient being rewritten to:

$$r_{012} = r_{01} + \frac{t_{01}t_{10}r_{12}\exp(-i2\beta)}{1 - r_{10}r_{12}\exp(-i2\beta)}. \quad (2.43)$$

The equation 2.43 can be reduced to a more simple equation using $r_{10} = -r_{01}$ and $t_{01}t_{10} = 1 - r_{01}^2$:

$$r_{012} = \frac{r_{01} + r_{12}\exp(-i2\beta)}{1 + r_{01}r_{12}\exp(-i2\beta)}. \quad (2.44)$$

The following Fresnel equation, reflectance and Snell's law for this model are expressed as:

$$r_{012,p} = \frac{r_{01,p} + r_{12,p}\exp(-i2\beta)}{1 + r_{01,p}r_{12,p}\exp(-i2\beta)} \quad r_{012,s} = \frac{r_{01,s} + r_{12,s}\exp(-i2\beta)}{1 + r_{01,s}r_{12,s}\exp(-i2\beta)} \quad (2.45)$$

$$R_p = |r_{012,p}|^2 \quad R_s = |r_{012,s}|^2 \quad (2.46)$$

$$N_0 \sin(\theta_0) = N_1 \sin(\theta_1) = N_2 \sin(\theta_2). \quad (2.47)$$

2.6 Fresnel equations for a multilayer model

In the previous sections, the Fresnel equations for two different models were evaluated. The Fresnel equations for a multilayer model is an amalgamation of the

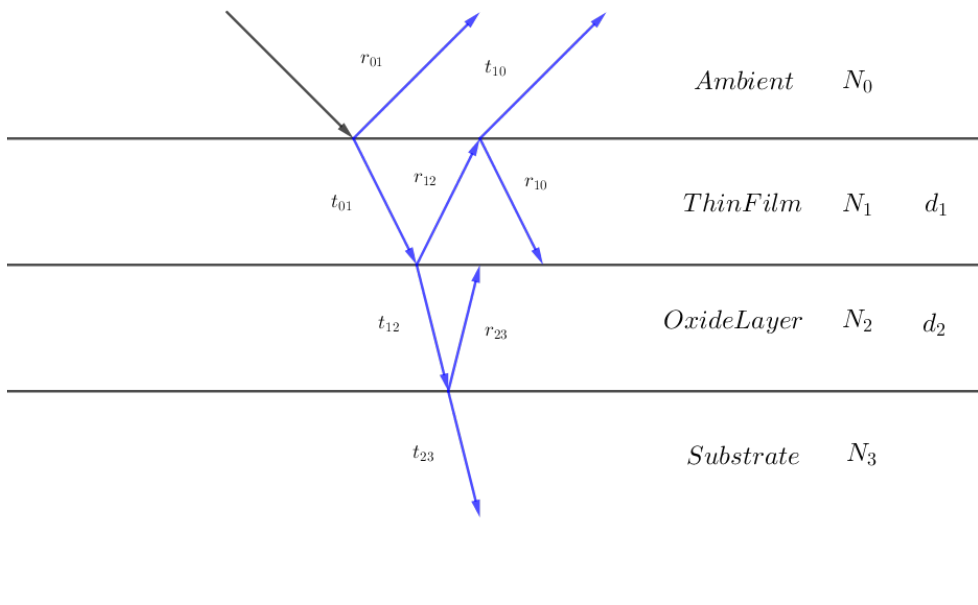


Figure 2.4: The model consists of the ambient, first thin film layer, second thin film layer and substrate. Each layer has a refractive index associated to it and both thin films have a thickness d_1 and d_2 respectively.

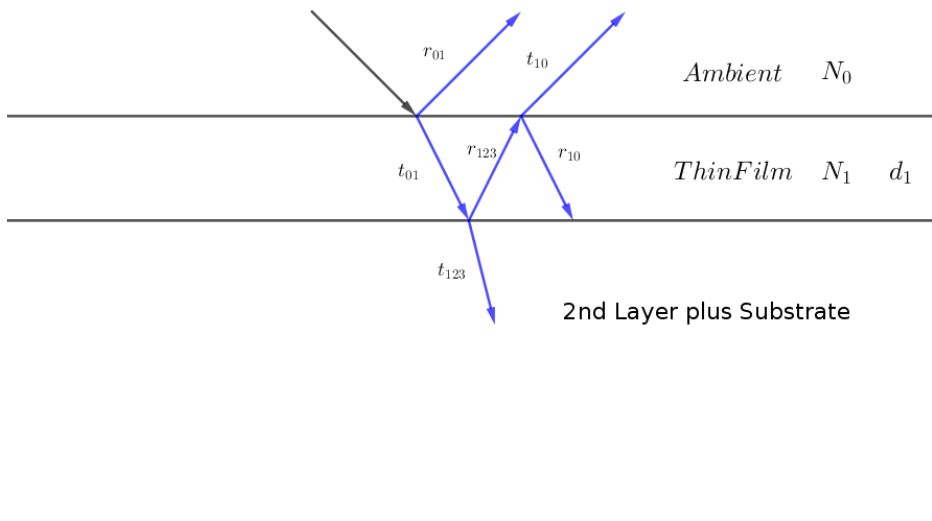


Figure 2.5: The model consists of the ambient, first thin film layer and second thin film layer plus substrate. The second thin film layer and substrate layer has been grouped together because r_{123} and t_{123} has been calculated the model seen in figure 2.4 and r_{0123} and t_{0123} can easily be calculated from this model. The ambient and first thin film layer have a refractive index and the first thin film layer has a thickness d_1 .

previous models. The reflection amplitude coefficient r_{123} for the multilayer model seen in the figure 2.4 with an ambient, two layers and a substrate can be calculated using equation 2.44. These equations produce the following expressions:

$$r_{123} = \frac{r_{12} + r_{23} \exp(-i2\beta_2)}{1 + r_{12}r_{23} \exp(-i2\beta_2)}. \quad (2.48)$$

β_2 is the phase variation in the second thin film layer with thickness d_2 . This is given as $\beta_2 = \frac{2\pi d_2 N_2 \cos(\theta_2)}{\lambda}$. The substrate and the layer on top of the substrate can be considered as one layer as seen in figure 2.5, thus the reflection amplitude coefficient and transmission amplitude coefficient is expressed as:

$$r_{0123} = \frac{r_{01} + r_{123} \exp(-i2\beta_1)}{1 + r_{01}r_{123} \exp(-i2\beta_1)}. \quad (2.49)$$

Inserting r_{123} into equations 2.49 gives the expanded Fresnel equation for this multilayer model:

$$r_{0123} = \frac{r_{01} + r_{12} \exp(-i2\beta_1) + [r_{01}r_{12} + \exp(-i2\beta_1)]r_{23} \exp(-i2\beta_2)}{1 + r_{01}r_{12} \exp(-i2\beta_1) + [r_{12} + r_{01} \exp(-i2\beta_1)]r_{23} \exp(-i2\beta_2)}. \quad (2.50)$$

2.7 Fresnel Equation Implementation

The fresnel equations have been implemented into matlab for model fitting and analysis of reflectance data. The optical fiber used in the spectral optical reflectance experiment is placed perpendicular to the thin film being measured. Thus the angle of incidence for the light is equal to zero, $\theta = 0$, and $\cos(\theta) = 1$. The p-polarisation fresnel equations and film phase thickness have been written into matlab as functions.

$$r_{jk} = \frac{E_r}{E_i} = \frac{N_k - N_j}{N_j + N_k} \quad (2.51)$$

$$\beta_i = \frac{2\pi d_i}{\lambda} N_i. \quad (2.52)$$

The matlab functions and complex refractive indices for the silicon substrate and silicon oxide layer can be found in appendix A.

Chapter 3

Experimental method

In this chapter a general outline of polymer classification will be outlined with the addition of a description of the polymers used in the solvent vapour annealing experiments. The spectrometer setup will be introduced and the necessary information related to how the spectrometer measures the reflectance of the thin films and the experimental measurement protocol. The reflectance data fitting will be explained and the chapter will close with a brief description of the solvent vapour annealing process.

3.1 Polymers

Polymers are long chains of molecular units called monomers, linked together by covalent bonds. Homopolymers are polymers built of one type of monomer repeating, where diblock copolymers are built up of two types of monomers, an A block and B block.

Polymers can also be expressed by the degree of polymerisation, N , which characterises the average number of mers units in the chain. It is defined as:

$$N = \frac{\bar{M}_n}{\bar{m}}, \quad (3.1)$$

where \bar{M}_n is the number average molecular weight and \bar{m} is the mer molecular weight. The polymerisation of a block co polymer is the sum of the individual block polymerisation, $N = N_A + N_B$. The number average molecular weight is defined as:

$$\bar{M}_n = \frac{\sum N_i M_i}{\sum N_i} = \sum x_i M_i, \quad (3.2)$$

where $x_i = \frac{N_i}{\sum N_i}$ is the fraction of the number of chains with a corresponding size range i and M_i is mean molecular weight in the size range i . The weight average

molecular weight for a polymer is defined as:

$$\bar{M}_w = \frac{\sum N_i M_i^2}{\sum N_i M_i}, \quad (3.3)$$

where N_i is the number of polymers with weight M_i . There is a dispersion of different polymer sizes in a solution, this dispersion is called the polydispersion index of the polymer and is expressed as:

$$PDI = \frac{\bar{M}_w}{\bar{M}_n}, \quad (3.4)$$

where \bar{M}_w is the weight average molecular weight and \bar{M}_n is the number average molecular weight [6].

The diblock copolymers can be further described by the volume fraction f that the different blocks take up and the Flory-Huggins interaction parameter χ which describes the degree of incompatibility between the two polymers. The volume fraction of A and B blocks are respectively:

$$f_A = \frac{V_A}{V_{total}} \quad f_B = \frac{V_B}{V_{total}}. \quad (3.5)$$

The Flory-Huggins interaction parameter is determine experimentally and expressed as:

$$\chi(T) = \frac{\chi_H}{T} + \chi_S, \quad (3.6)$$

where χ_H is of due to enthalpy and χ_S is due to entropy. Chemically dissimilar polymers tend to display a larger χ value than chemically similar,[7][8].

Polymer are found in different physical states, the most common being in a glass or rubber state. A glassy state is described as amorphous since the structure resembles both a liquid and a solid and this state is found below the polymers glass transition temperature T_g . A polymer can melt into a viscous state, this state is its rubber state. This state is found above the polymers glass transition temperature [9].

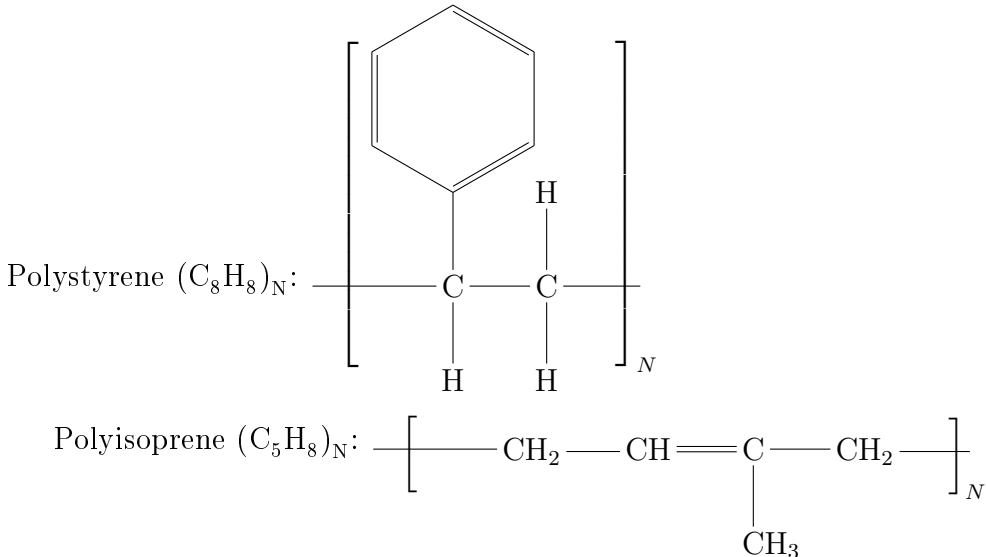
Micro-phase segregation of block copolymers is seen and understood as a thermodynamic process, in which the blocks of the polymer have a thermodynamic incompatibly described by Flory-Huggins interaction parameter χ_{AB} , which creates a nanoscale structure. The covalent bond between block A and block B prevent macrophase separation, and micro-phase segregation occurs. This leads to the application of block copolymers as self-assembling structures which can be used nanolithography and as templates in photonics. The block copolymers self-assembling properties depend on the mobility of the polymer chains before structural reorganisation can

proceed. This is normally done by thermal treatments above the polymers glass transition temperature T_g , but with high molar mass system long annealing times are need [10].

3.2 Polymers used in Solvent Vapour Annealing

In this section the homopolymers Polystyrene and Polyisoprene and the block copolymer Polystyrene-b-Polyisoprene properties will be presented.

3.2.1 Homopolymer Chemistry



3.3 Polymer Considerations

Before commencing solvent vapour annealing some consideration is need into what polymers, what solvent and what substrate should be used. Polystyrene has been chosen as block A of the block copolymer and Polyisoprene chosen as block B. Polystyrene is in the glassy phase at room temperature, where polyisoprene is in a rubbery phase at room temperature. The morphology of the block can shed a light on how the vapour could interact with the blocks during solvent vapour annealing. The molar mass, polymerisation of both block, polydispersion index and the interaction parameter between the two block is helpful to understand what might happen during the solvent vapour annealing process. High molar mass systems are strongly segregated and take longer to come into equilibrium than a lower molar mass system. Interaction between the solvent and the polymers will also give insight into how the morphology could evolve during the solvent vapour annealing.

3.3.1 Relevant values

Polymer Values			
	Polystyrene	Polyisoprene	PS-b-PI
T_g	379 K	204 K	
N			
N_A			
N_B			
f_A			
f_B			
\bar{M}_n			
\bar{M}_w			
PDI			
χ			
n	1.60	1.51	

3.3.2 List of polymers used in experiments

Polymer used in experiments						
Experiment	Polymer	ID	Spincoat Thickness	Static Measurement	Static Thickness	Refractive Index
Light Source Fluctuation	Polystyrene	349	≈ 200 nm	280.4 nm	1.5944	
SVA Ambient Study	Topsil Blank	N/A	N/A	N/A	N/A	
Polystyrene Swelling	PS	348	≈ 200 nm	275.5 nm	1.5975	
Polyisoprene Swelling	PI	353	≈ 200 nm	301 nm	1.4594	
Polystyrene-b-Polyisoprene	PS-b-PI	370	≈ 100 nm	97.3 nm	1.5659	

3.4 Spin Coating thin films

Spin coating is the deposition method used to fabricate the thin films used in this thesis. This is a wet method where a polymer is dissolved in a solution then deposited onto the semiconductor wafer, silicon wafer. The silicon wafer is rotated at a fixed

low rpm to spread the polymer solution across the wafer. The rpm is increased spinning off the excess solution and will evaporate leaving a thin film with uniform thickness. This method is predicted by the following expression:

$$d = \left(\frac{\eta}{4\pi\rho\omega^2} \right)^{\frac{1}{2}} t^{-\frac{1}{2}}, \quad (3.7)$$

where d is the predicted thickness, η the viscosity coefficient of the polymer solution, ρ solution density, ω angular velocity of the spinning and t is the spinning time [9]. The spin coated block copolymers show defect-rich morphologies due to fast evaporation of the solvent and the polymers being in a thermal non-equilibrium [11].

3.5 Spectrometer Setup

The experimental setup is comprised of a NanoCalc XR and a Halogen light source(HL-2000-FHSA) seen in figure 3.2, which can produce wavelengths of 360 nm to 2400 nm. When the samples are being measured they are either placed on the ocean optics single point stage seen in figure 3.3 or in the solvent vapour annealing (SVA) experimental chamber seen in figure 3.4 made by the IMFUFA(Indsatsområdet for Studiet af Matematik og Fysik samt deres Funktioner i Undervisning, Forskning og Anvendelser) workshop for small angle x-ray scattering (SAXS) and grazing incidence small angle x-ray scattering(GISAXS) experiments. The NanoCalc is comprised of a spectrometer and an internal light source as seen in the figure 3.5, which can produce wavelengths of 250 nm to 1050 nm and measure thicknesses of 10 nm to 100 μm . The NanoCalc XR is connected to a computer where the NanoCalc software is installed and operated. For the experiments the halogen light source is used since it has a larger output power then the internal light source of the NanoCalc XR. The larger intensity output is need when performing experiments in the SVA experimental chamber. The lid of the SVA experimental chamber holds the optical fiber and light passes through a sapphire lens before entering the chamber and illuminate the thin film. The sapphire lens is need to focus the light upon the thin film due to the distance from the optical fiber to the sample is greater than the single point stage. Throughout this thesis "with optics" will be used when referring to measurement taken using the SVA experimental chamber since the light passes through the sapphire lens. "Without optics" refers taking measurements using the single point stage.

For experiments done in this thesis white light is produced in the light source(HL-2000-FHSA), which travels through optical fiber and strikes that sample. The re-

flected light travels back through the optical fiber and the intensity across every wavelength of the white light is collected in the spectrometer and is sent to software created by in house and saved to a file and analysed in MATLAB®.

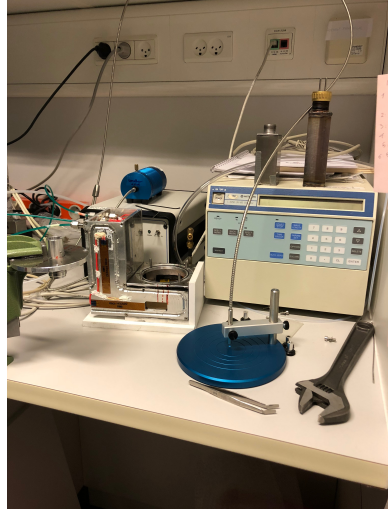


Figure 3.1: SVA experiment area

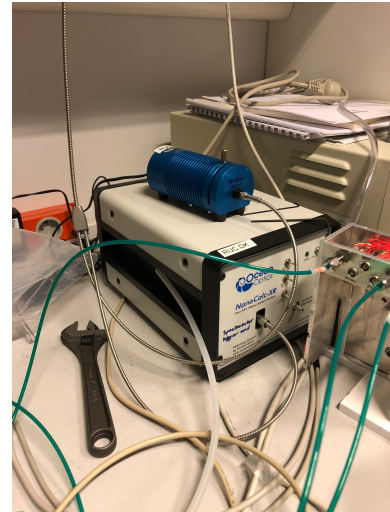


Figure 3.2: NanoCalc XR and a Halogen light source(HL-2000-FHSA)

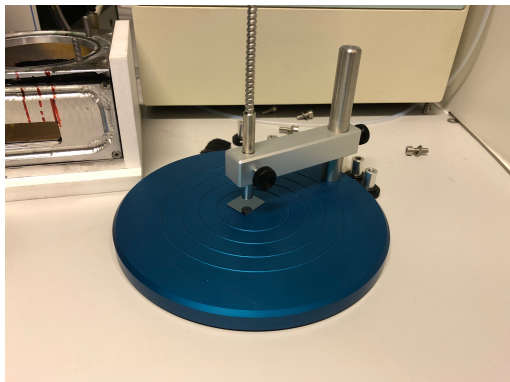


Figure 3.3: Single point stage

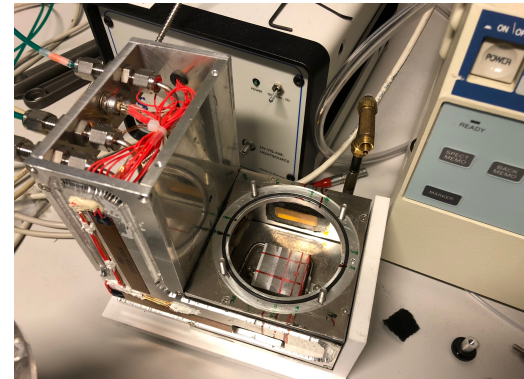


Figure 3.4: SVA experimental chamber minus lid

3.6 Reflectance measurements in the NanoCalc spectrometer

The NanoCalc spectrometer measures three light intensities which will be called a measurement onwards. The three measurements are the dark measurement (dark), the reference measurement (ref) and the thin-film measurement (meas). The dark measurement is the amount of light received by the optical fiber from external

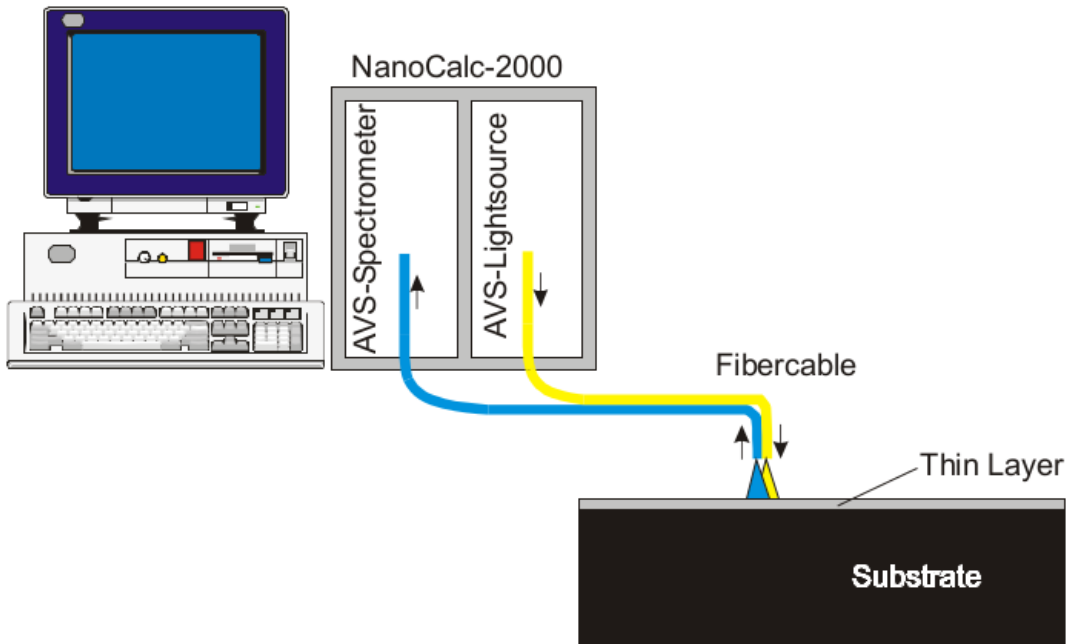


Figure 3.5: This figure describes the NanoCalc set-up and has been taken from [12]. Light from a light source travels down the optical fiber illuminating the sample. The reflected light is collected by the optical fiber and analysed in the spectrometer. The spectrometer is connected to the computer by USB and the data is stored, modelled and manipulated through the NanoCalc software.

sources. The reference measurement is the amount of light reflected from a blank silicon wafer and the thin film measurement is the amount of light reflected from the sample. From chapter 2.3, the reflectance of a sample can be expressed as :

$$R_{sample} = \frac{I_{sample}}{I_{incident}}. \quad (3.8)$$

The spectrometer does not measure the intensity of the incident light, therefore the reflectance of the substrate is used to isolate the incident light intensity and inserted into equation 3.8. The reflectance of the substrate is used because it is easily calculated using the Fresnel equations as described in chapter 2.4.

$$R_{ref} = \frac{I_{ref}}{I_{incident}} \quad (3.9)$$

$$\Rightarrow I_{incident} = \frac{I_{ref}}{R_{ref}}. \quad (3.10)$$

Inserting equation 3.10 in equation 3.8, the reflectance for the sample is expressed without the incident light intensity as:

$$R_{sample} = \frac{I_{sample}}{I_{ref}} \cdot R_{ref}. \quad (3.11)$$

The reflectance of the sample is given as:

$$Reflectance = \frac{Meas - Dark}{Ref - Dark} \cdot R_{sub}. \quad (3.12)$$

This is the same expression given in the NanoCalc spectrometer manual [12]. Through reproduction of the data and curves given by the NanoCalc spectrometer, i can deduce that the reference measurement has already had the dark measurement subtracted, giving the following reflectance expression:

$$Reflectance = \frac{Meas - Dark}{Ref} \cdot R_{sub}. \quad (3.13)$$

Placing equation 3.13 equal to the reflectance equations using the Fresnel equations from chapters 2.4, 2.5 and 2.6, the NanoCalc spectrometer software can fit a thickness of the sample.

3.7 Reflectance measurement protocol

In this section the experimental protocol for both taking measurements without the optics and with the optics are given. The halogen light source has been turned on 30 minutes prior to taking the measurements and the thin films have had 30 minutes to

climatise to room temperature. The single point stage is set up and tested using a reference step wafer of known thicknesses. The protocol will be formulated in steps.

3.7.1 Without Optics

1. Take a continuous reference measurement and adjust the light intensity, such that the reference measurements maximum is 50% of the y-axis.
2. Clear the reference measurement.
3. Take the optic fiber and point it away from anything that can reflect light.
Take a dark measurement.
4. Place the optic fiber into ocean optics single point stage. The optic fiber is positioned 4mm above the single point stage.
5. Place a blank silicon wafer under the optic fiber and take a reference measurement.
6. Save the dark and reference measurement.
7. Place a thin film under the optical fiber and take a measurement.

3.7.2 With Optics

1. Take a continuous dark measurement with the optic fiber with a dark cloth in the optics where the thin film would lie and adjust the light intensity, such that the dark measurements maximum is at 100% of the y-axis.
2. Clear the dark measurement.
3. Take the optics as a whole and point it away from anything that can reflect.
Take a dark measurement.
4. Place a blank silicon wafer into the test chamber and place the optics into the test chamber. Take a reference measurement.
5. Save the dark and reference measurement.
6. Take the optics off the test chamber, remove the blank silicon wafer and place in a thin film sample. Place the optics onto the test chamber. Take a measurement.

3.8 Fitting of the reflectance data

The mean square error is used when fitting the Fresnel equations to the reflectance measurements. The mean square error is given by:

$$MSE = \frac{1}{n} \sum_{i=1}^n (Y_i - \hat{Y}_i)^2, \quad (3.14)$$

where n is equal to the amount of data points used, Y_i is the measured value and \hat{Y}_i is the estimated value. The fitting range is from 450 nm to 900 nm. This range has been chosen ...[ARGUMENT HERE]. The parameters used in the fitting of Fresnel equations are the ambient refractive index n_0 , the thin film refractive index n_1 and the thin film thickness d_1 . The thickness for the silicon oxide layer is fixed at 2 nm and the complex refractive index values at each wavelength has been taken from Ocean Optics software. The complex refractive index for the silicon substrate has also be taken from the Ocean Optics software. Both the refractive indices for ambient and thin film are fitted for real numbers. The fitting scripts loops through the three parameter arrays calculating the mean square error for the measured reflectance data, finds the smallest mean square error value and saves the three parameters associated the smallest mean square error into an array. The next reflectance measurement is loaded in and the process begins again.

3.9 Bronkhorst mass flow meters

To regulate the solvent vapour annealing process, the experimental setup includes three Bronkhorst mass flow meters. This is important since controlling the vapour flow in different ways changes the structuring of the polymers when swelling. One EL-Flow select(F-201CV-500) with a flow capability for N_2 of 4 ml min^{-1} to 750 ml min^{-1} , or 400 SCCM (Standard centimetre cubed per minute at 1 atm and 273 K). Two EL-Flow select(F-201CV-200) with a N_2 flow of 1.6 ml min^{-1} to 300 ml min^{-1} , or 200 SCCM (Standard centimetre cubed per minute at 1 atm and 273 K) [13].

During the both swelling processes, the SCCM will be kept constant to 200 SCCM, with the assumption that the flowrate is constant through the system. When nitrogen flows through the bubbler and solvent the flowrate will change and thus the pressure in the SVA chamber will change.

3.10 Solvent Vapour Annealing Process

The solvent vapour annealing process is divided into two process, a swelling and a drying process. In the swelling process a dry polymer upon a wafer is placed into the annealing chamber and is subjected to nitrogen gas. Slowly nitrogen gas is decreased and nitrogen gas through a bubbler filled with a solvent, in this thesis toluene, is increased creating vapour in the annealing chamber. When performing SVA, a solvent is chosen that is either neutral or slightly selective towards one of the polymers in the block copolymer. Solvent uptake is also dependant on the physical state of the block copolymer and the block fraction volume. The thin film will swell due to thermodynamic driving forces associated with the entropy of mixing of vapour and polymer blocks. The swelling will continue until the chemical potential of the vapour and the solvent in the thin film is in equilibrium. A diffusion front will arise continuing through the thin film from the vapour interface through to the substrate. It is published that the vapour pressure is an important thin film thickness parameter and should be controlled throughout the annealing. The vapour pressure is dependant on the mass flow controller, temperature of the solvent and temperature of the annealing chamber. The time taken to fully swell is also dependant on how organised the dry thin film is before swelling, this leads to varying swelling time. In a solvent swollen state the mobility of the polymer chains increase and the polymer can move in the volume of the thin film. The molar mass of the polymer plays a role in the how fast the polymer self assembles and a equilibrium state may not be achieved during the swelling. In the drying step the nitrogen gas flow through the bubbler is decrease and the direct nitrogen gas flow is increased. The solvent in the thin film is evaporated and the rate in which the solvent evaporates has been seen to have an impact of the nanoscale structure, in effect of quenching an organised structure. It is documented that both fast and slow evaporation leads to organised structure in block copolymers. An ordering front forms in the thin film during the evaporation where the thin film show order closer to the vapour interface and as the front propagates through the film, order follows in its wake[10].

Structure characterisation is important during the stages of solvent vapour annealing, different experimental method illuminate different parameters. Optical Spectral reflectometry used in this thesis will investigate how the thickness of the thin film evolves during SVA and shed light on how the refractive index for the ambient and thin film could evolve.

3.10.1 Solvent vapour annealing protocol

The solvent vapour annealing protocol used is a slow swell up to maximum toluene vapour flow which takes $5500\text{ s} \approx 92\text{ min}$ and a slow deswell which is the reverse of the slow swell up to the maximum taking $4000\text{ s} \approx 67\text{ min}$ to fully dry back roughly the thin films start thickness. The SVA takes a total of 158 min to run. The slow swell is broken up into five regions, the first region channel 1 dry nitrogen gass (400SCCM) is set to 50% for 1000 s. In the second region, channel 1 drops to 37.5% and channel 2 which flows through the bubbler increases from 0% to 25% for 1000 s. The third region, channel 1 drops to 25% and channel 2 increases to 50% for 1000 s. The fourth region, channel 1 drops to 12.5% and channel 2 increases to 75% for 1000 s. The fifth region, channel 1 drops to 0% and channel 2 increases to its maximum 100% for 1500 s. The solvent concentration can be calculated by the solvent loading of the thin film though the volume concentration, which can be expressed using the thickness. The solvent concentration is expressed as:

$$\phi = \frac{V_{solvent+film} - V_{film}}{V_{solvent+film}} = \frac{t_{solvent+film} - t_{film}}{t_{solvent+film}} = 1 + \frac{t_{film}}{t_{solvent+film}}, \quad (3.15)$$

where V is the volume of the thin film, and t is the thickness of the thin film [14].

During the solvent vapour annealing protocol a reflectance measurement is taken every 10 seconds and saved into its own .dat file. The solvent vapour annealing protocol is controlled by a script loading into the Bronkhorst Flowplot software. The script is called slowslow.fps and has been included in the appendix B.1 of this thesis.

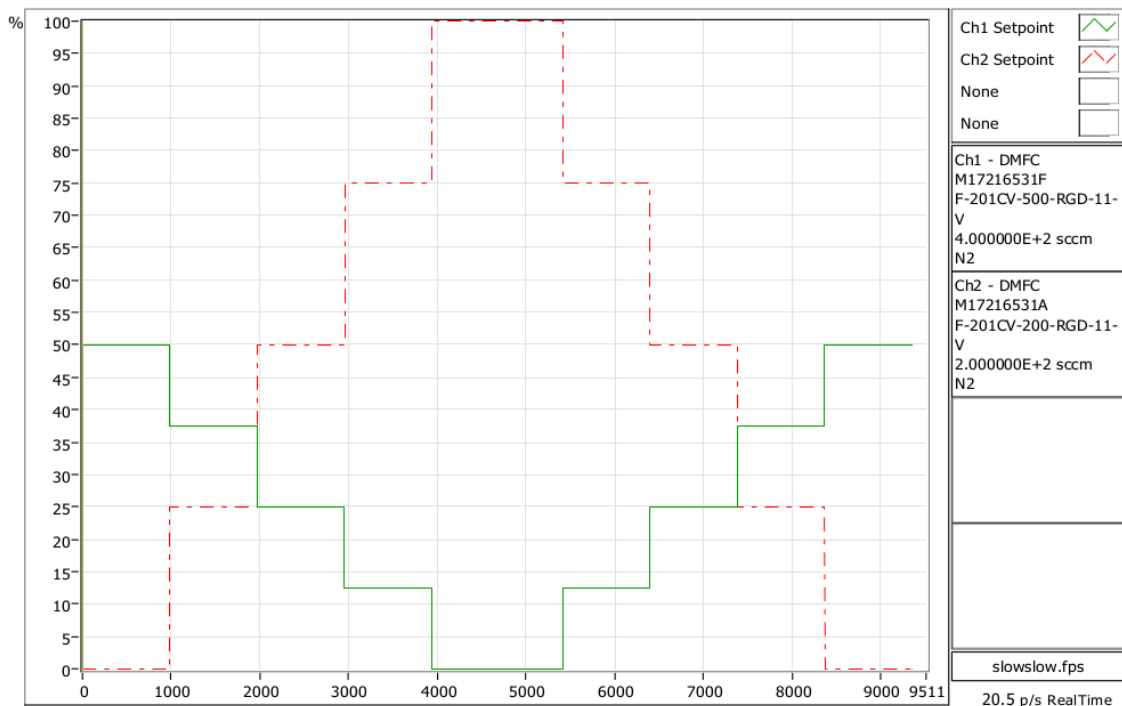


Figure 3.6: Slow swelling and slow deswelling protocol. Along the x-axis, time is shown in seconds, the full SVA protocol taking 9500s. Along the y-axis, how hard the mass flow meter is working in procent. The green plot belongs to the 400SCCM Bronkhorst mass flow meter controlling the nitrogen gas and the red dashed plot belongs to the 200SCCM Bronkhorst mass flow meter controlling the nitrogen flowing through the bubbler. The swelling is done by loading a swelling script called `slowslow.fps` show in appendix B.1.

Chapter 4

Analysis

4.1 Light source fluctuation

Looking at equation 3.13, which is the expression for how the spectrometer measures the reflectance of light from the thin films reveals the importance of the intensity of light being used in the measurement. A fluctuation in the intensity of light gives repercussions for the reference measurement and dark measurement taken as both measurements are not correct at the point they were taken and will not correct in future measurements. The question is how long does a reference and dark measurement remain valid. This study aims is to shed light on this problem. The scripts used can be found in appendix B.2. The thin film used is polystyrene and a total of 14 measurements were done in the SVA experimental chamber. A measurement was taken every 30 min, a measurement was made manually at 10:47 and the automatic measurements commenced at 11:19. The measurements can be seen plotted together in figure 4.1. Distinguishing which curve belongs to which time is not possible because of the limited amount of plotting colours, but two groups of reflectance curves can be seen at the 600 nm mark and again at the 900 nm mark.

Figures 4.2 and 4.3 show the first reflectance measurement taken at 10:47 plotted against the reflectance measurements taken at the times 12:19, 13:49, and 15:19, 17:19 respectively. In figure 4.2, the reflectance measurements lie close to one another. In figure 4.3, the drop in reflectance seen at the 600 nm mark starts at the time 15:19 and continues onwards.

The reflectance difference has been plotted in figure 4.4. It can be seen that the difference of 10:47 plotted with both 12:19 and 13:49 lie on top of one another and the difference of 10:47 plotted with both 15:19 and 17:49 lie on top of one another. There is a clear difference between the two groups of plots.

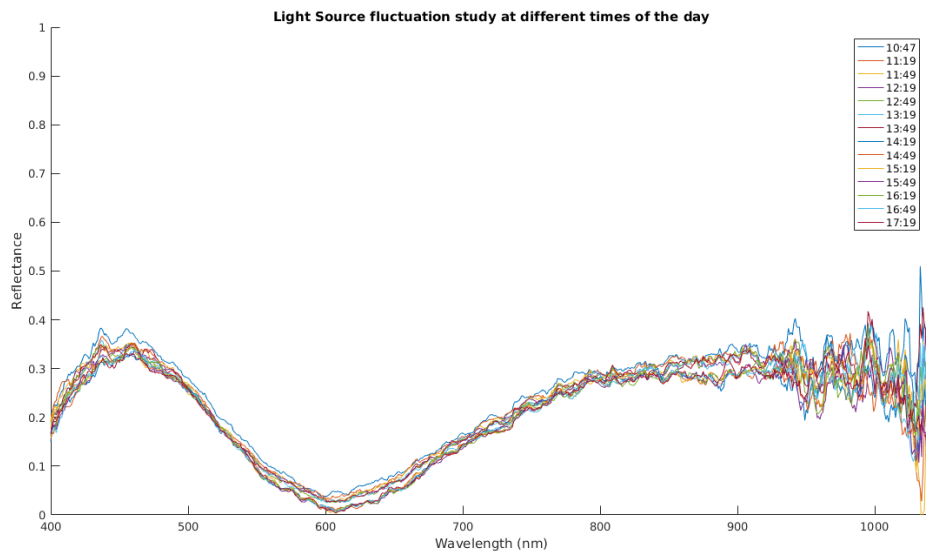


Figure 4.1: 14 reflectance measurements plotted representing a reflectance measurement taken every 30 minutes. Distinguishing which curves belongs to which time is not possible, but two groups of reflectance curves can be seen at the 600 nm mark and again at the 900 nm mark.

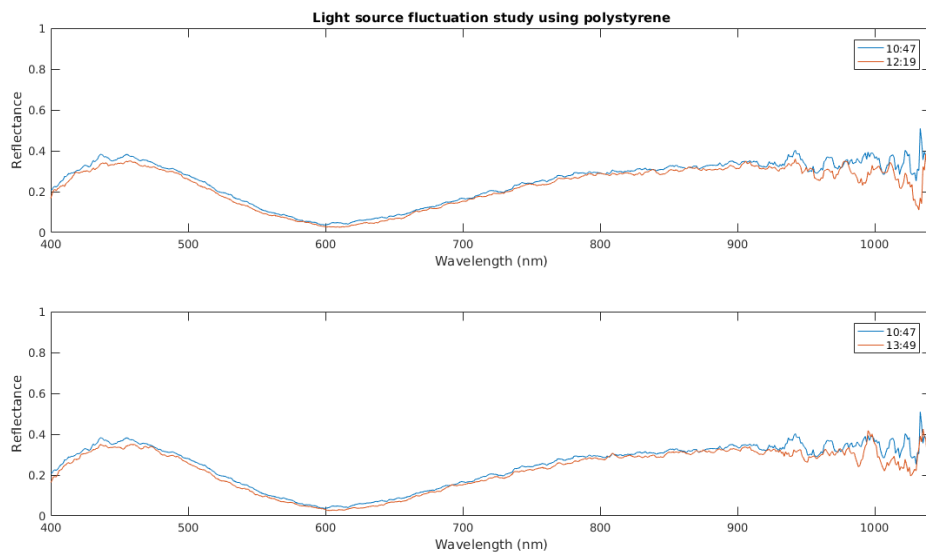


Figure 4.2: The reflectance measurement taken at 10:47 plotted with both 12:19 and 13:49. It can be seen that there is a small deviation but lay close to one another.

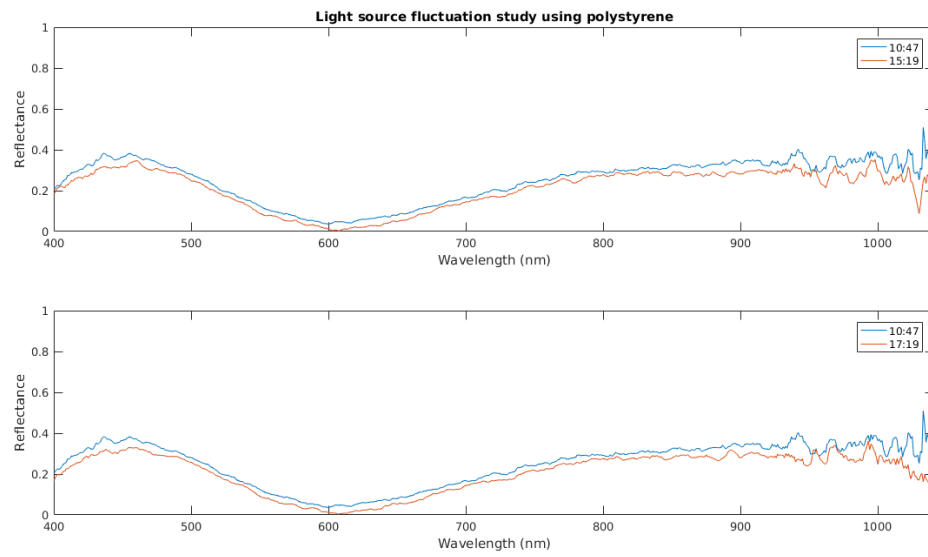


Figure 4.3: The reflectance measurement taken at 10:47 plotted with both 15:19 and 17:49. It can be seen that the deviation between the reflectance data is increasing.

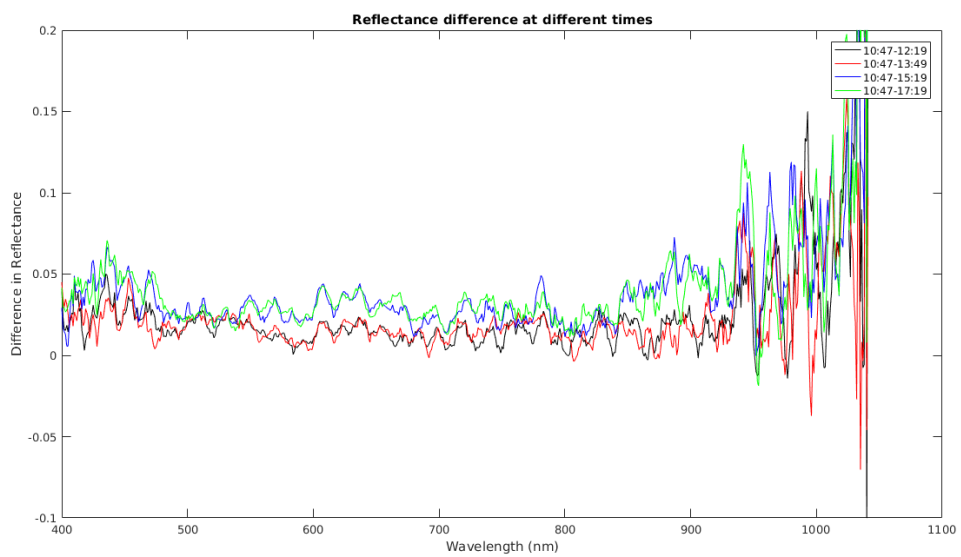


Figure 4.4: The reflectance difference between the reflectance data at 10:47 and the other times 12:19, 13:49, 15:19 and 17:19 are shown. It can be seen that the reflectance data groups itself into two, first group with times 12:19 and 13:49 and the second group 15:19, 17:19.

The conclusion to this study is that there is a 3 hour window where the variation in the intensity from the light source does not impact the reflectance measurements. Beyond the 3 hour period, the reflectance difference increases and can impact the reflectance measurements.

4.2 Nano-Calc Simulated Reflectance Curves

The Nano-Calc software does not go into detail how it models and analyses the reflectance curves, a little study was need to understand the process better and test if the software uses Fresnel equation and if the functions written by myself could reproduce these curves. Using the Nano-Calc software, simulated reflectance curves were produced from three models. The first model consists of of ambient of air refractive index 1, and the silicon substrate, the Fresnel equation can be seen in equation 2.31. The reflectance curves can be seen in figure 4.6. The second model consists of ambient of air refractive index 1, a thin film of polymer with homogeneous refractive index 1.5 and thickness 1000 nm and the silicon substrate, the fresnel equation can be seen in equation 2.44. The reflectance curves can be seen in figure 4.7. The third model consists of ambient of air refractive index 1, a thin film of polymer using the Cauchy dispersion equation $A = 1.4450$, $B = 3 \cdot 10^4$ and $C = 4 \cdot 10^7$, a silicon oxide layer with thickness 2 nm and the silicon substrate, the fresnel equation can be seen in equation 2.49 . The reflectance curves can be seen in figure 4.8. The Cauchy dispersion equation is an empirical equation describing how the refractive index varies with respect to wavelength. The Cauchy dispersion equation is defined as:

$$n(\lambda) = A + \frac{B}{\lambda^2} + \frac{C}{\lambda^4}, \quad (4.1)$$

where λ is the wavelength. This is the only time the Cauchy dispersion equation will be used. The coefficient A describes the refractive index when the terms with wavelength become less dominant. The Cauchy dispersion equation has not been implemented into the fitting protocol used on the reflectance data of the homopolymers and block copolymer. It is interesting nonetheless to look at the refractive index of the polymers as a function of wavelength. The cauchy dispersion equation has been plotted in figure 4.5. The coefficient have been found experimentally using ellipsometry. It can be seen in figure 4.5 that polystyrene is the only polymer which is close to a constant refractive index. Polyisoprene and polystyrene-b-polyisoprenes refractive index diverges alot compared to the constant refractive index. Since the fitting of the homopolymers and Block copolymer reflectance data is done across the

interval [450, 900], i have included the amount in which the refractive index deviates from the constant refractive index at 450 nm in red font.

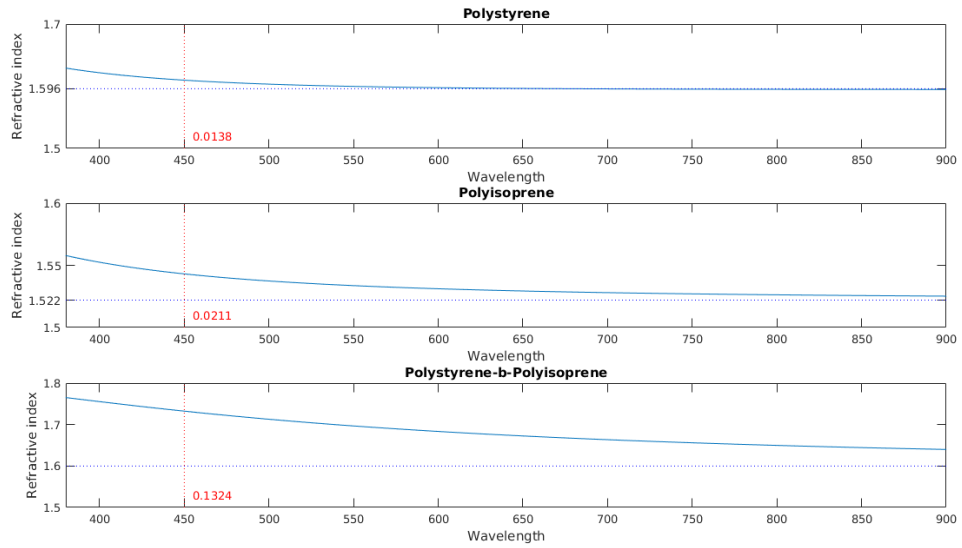


Figure 4.5: The cauchy dispersion equation has been plotted for Polystyrene, Polyisoprene and Polystyrene-b-Polyisoprene. The amount in which the refractive index deviates from the constant refractive index at 450 nm has been included in red font.

When modelling the Fresnel equations, both the refractive index and absorption index for the silicon oxide layer and silicon substrate have been used for the complex refractive index. The dispersion for both the silicon oxide layer and silicon substrate have been taken from the Nano-Calc software and the graphs and script to produce the graphs can be seen in appendix A.2.

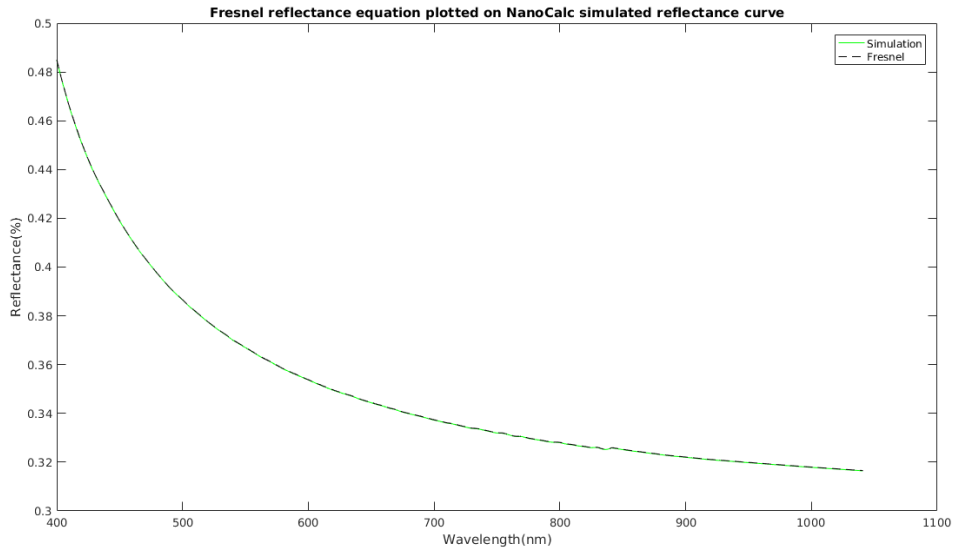


Figure 4.6: Simulated curve of the model plotted with the green curve, consists of ambient of air refractive index 1, and the silicon substrate. The Fresnel equations plotted with the black dashed curve consists of the same model. It can be seen that the two curves fall upon each other.

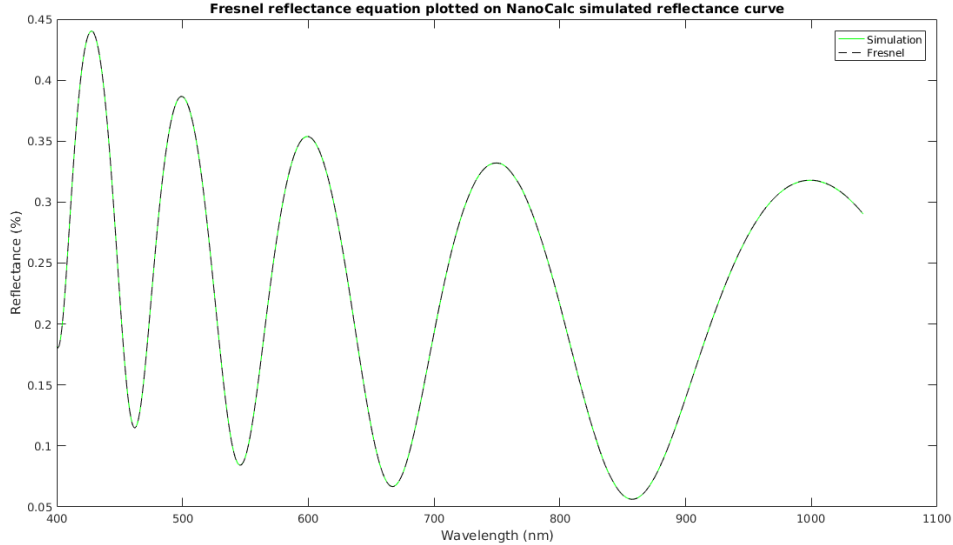


Figure 4.7: Simulated curve of the model plotted with the green curve, consists of ambient of air refractive index 1, a thin film of polymer with homogeneous refractive index 1.5 and thickness 1000 nm and the silicon substrate. The Fresnel equations plotted with the black dashed curve consists of the same model. It can be seen that the two curves fall upon each other.

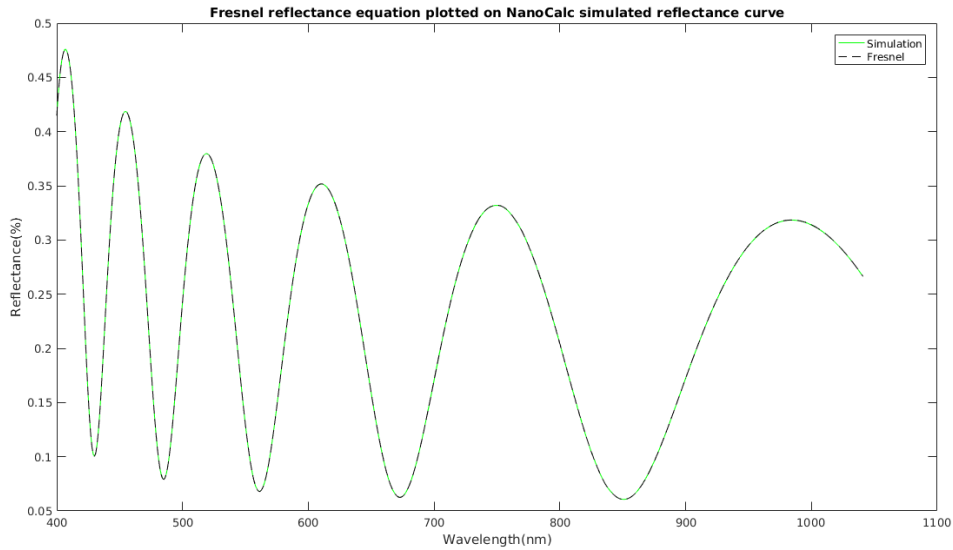


Figure 4.8: Simulated curve of the model plotted with the green curve, consists of ambient of air refractive index 1, a thin film of polymer using the Cauchy dispersion equation $A = 1.4450$, $B = 3 \cdot 10^4$ and $C = 4 \cdot 10^7$, a silicon oxide layer with thickness 2 nm and the silicon substrate. The Fresnel equations plotted with the black dashed curve consists of the same model. It can be seen that the two curves fall upon each other.

Two conclusions have been drawn from this study. The first is that the Fresnel equations implemented by myself in the script used in this chapter can reproduce the simulated curves used by the Nano-Calc software to model the reflectance curves. The second is that the fitting protocol for the reflectance curves will not implement the Cauchy dispersion for refractive index because it is not fully understood and it is not something the optical spectral reflectance method can fully reveal.

4.3 Solvent vapour annealing ambient study

During solvent vapour annealing, nitrogen flow through the bubbler increases, increasing the toluene vapour present in the chamber. The question arises, does the refractive index of the ambient increase with the increase of toluene vapour available in the chamber. A blank silicon wafer has been used for this study. Upon the silicon wafer lies a silicon oxide layer modelled to have a thickness of 2 nm. The refractive index has been allowed to vary between 1 through to 2 with a step of 0.1. The fitting protocol loops through each refractive index, calculating the theoretical reflectance curve from the fresnel equation 2.31. The mean square error has been calculated for each loop and the minimum has been found and the refractive index

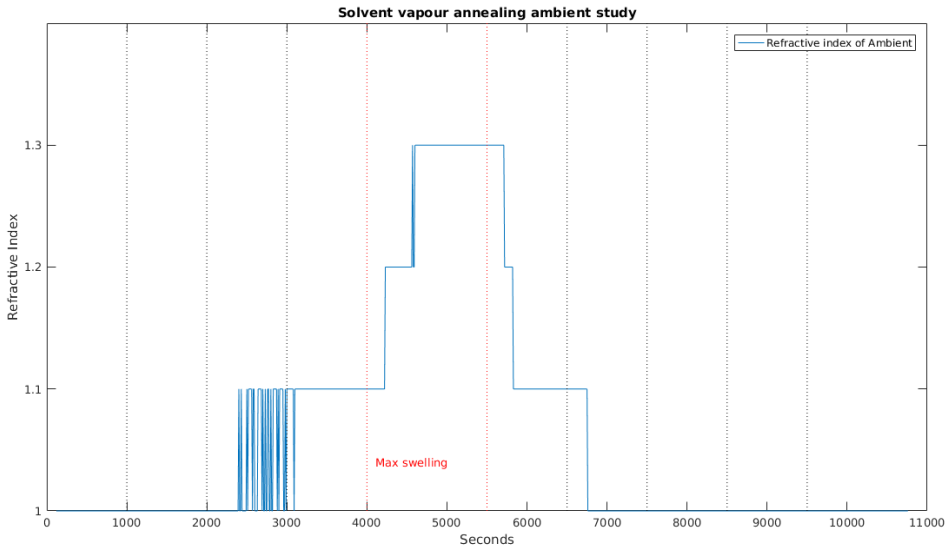


Figure 4.9: The refractive index of the ambient has been plotted. The refractive index has been fitted by plotting the theoretical reflectance curve from the fresnel equation 2.31 and calculating the mean square error. The refractive index from the lowest mean square error has been used per reflectance measurement. The dotted vertical lines represent the swelling and deswelling step outlines in section 3.10.1. The red dotted lines indicate the period where there is maximum flow through the bubbler.

saved into a file. The swelling protocol used has been outlined in section 3.10.1 and can be seen in figure 3.6. From the mean square error fitting, the refractive index varied between 1 through to 1.3 through the course of swelling, this can be seen in figure 4.9. The dotted vertical line represent the different stages in the solvent vapour annealing and the maximum flow through the bubbler has been highlighted with the red vertical dots.

The mean square error for each reflectance measurement is shown in figure 4.10. It can be seen between the 2000 and 3000 second mark the refractive index is erratic, this is mirrored in the increase in the mean square error. The same happens when the fitting increases the refractive index to 1.3, the mean square error increase then falls. During the deswelling period there is an increase in mean square error when every the refractive index decreases. When watching the reflectance data play like a movie, it can be seen that the reflectance does decrease. The decrease in reflectance data is shown in figure 4.11. As stated the wafer used is a silicon wafer with an oxide layer. Both layer are unable to take up vapour and their thickness cannot increase, thus the variable in this set up is the ambient refractive index.

The conclusion to this study is that the ambient in the solvent vapour annealing

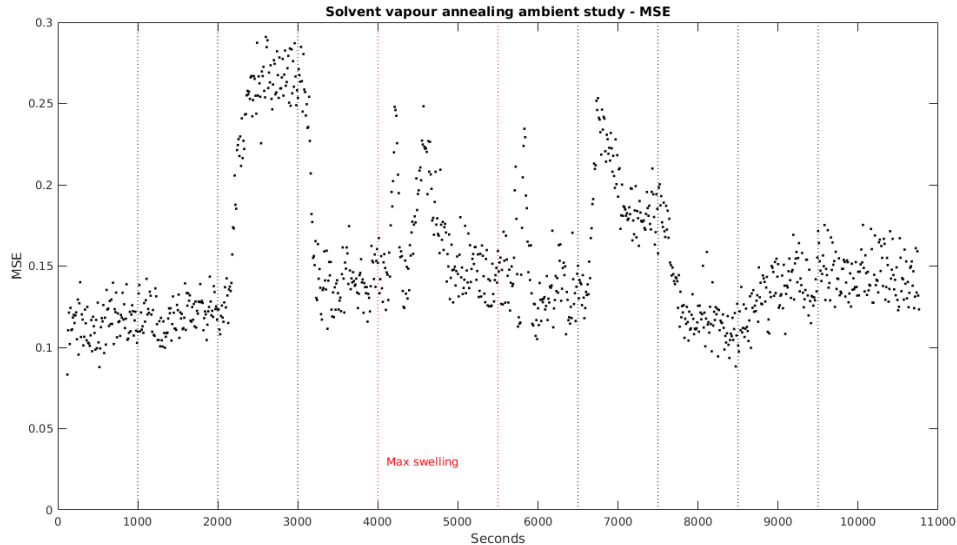


Figure 4.10: The mean square error has been plotted as a function of time. The frames have been captured every 10 time. It can be seen that the error increase every time the modelling increases or decreases the refractive index but stabilises back to a level close error before the change in refractive index.

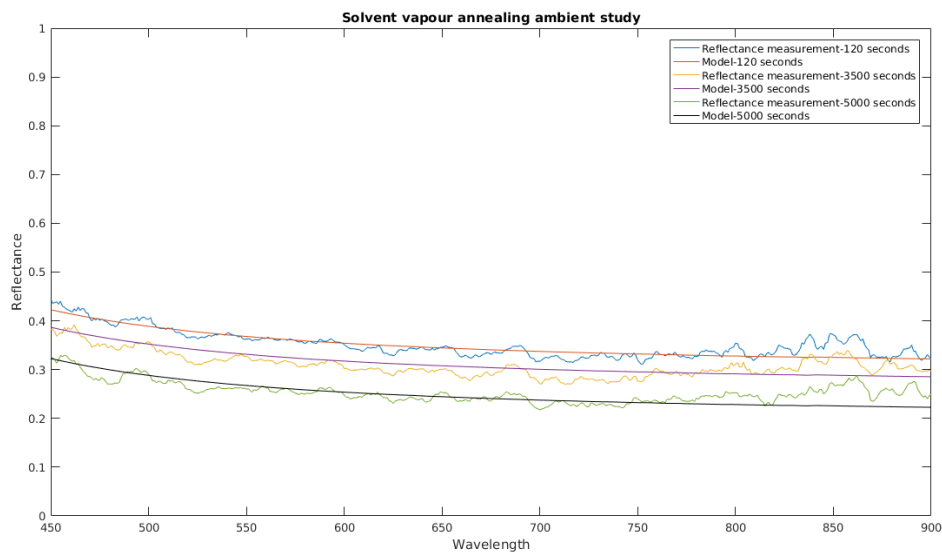


Figure 4.11: Three reflectance curves has been plotted to show how the reflectance decreases during solvent vapour annealing when the toluene vapour in the chamber increases. The fresnel reflectance model equation 2.31 has been plotted for each stage in the solvent vapour annealing. The measurement at time 120 second is modelled with a refractive index of 1. The measurement at time 3500 time is modelled with a refractive index of 1.1. The third measurement at time 5000 time is modelled with a refractive index of 1.3.

chamber increase during the swelling. The interval in which the refractive index of the ambient increase, lies between 1 and 1.3.

4.4 Polystyrene

Polystyrene with a measured thickness of 275.5 nm and a refractive index 1.5975 using the single point stage, has been placed into the solvent vapour annealing chamber and swelled using the swelling protocol outlined in section 3.10.1. The ambient refractive index has been bounded to the interval [1, 1.3] with a step size 0.1 and the thin film refractive index bounded to the interval [1.1, 2] with a step size 0.1. The thin film thickness has been bounded to the interval [250 nm, 600 nm] with step size 1 and the silicon oxide thickness set to 2 nm. Figure 4.12 shows the values found using the fitting protocol outlined in section 3.8. The vertical dotted lines have been added to represent times where the swelling protocol has increased and decreased the nitrogen gas flow and toluene vapour. Horizontal lines have been added to the thickness plot to help the reader. The thickness of the polystyrene shows a slow uptake of the toluene vapour during the first 4000 seconds. The thickness increases from 275 nm to 300 nm. During this time the polystyrene refractive index increases from [1.6] to [2.0]. The polystyrene refractive index jump from 1.6 to 1.7 passed the 1000 seconds mark and the jump from 1.8 to 2 around the 3000 second mark coincide with jumps in the ambient refractive index. The refractive index of the ambient increases slowly over the course of the first 4000 seconds, which coincides with the increased flow of nitrogen through the toluene. There are areas in the figures where there is noise. The noise manifests itself through back and forth jumps in the refractive index values and jumps in the thickness values. The fitting has trouble around the 450 nm and 500 nm interval, i believe this is the cause of the noise. This is also reflected in the mean square error figure 4.13. The increase of the mean square error at 1500 mark coincides with the noise in the refractive index of the ambient and thin film, and thickness, figure 4.12. The increase of the square error at 2500 and 3000 mark shows sudden drops in the thickness values which also coincide with increase of the refractive index of the thin film. During the maximum swelling interval the mean square error increases from 0.1 to 1. The reflectance during this time decreases creating a gap between the fresnel equations and reflectance measurement, increasing the mean square error. When the slow drying commences at the 5500 second mark, the thickness and mean square error values drops significantly. The swelling from 300 nm to 450 nm takes roughly 1500 seconds and deswelling to roughly the same thickness takes 500 seconds. The

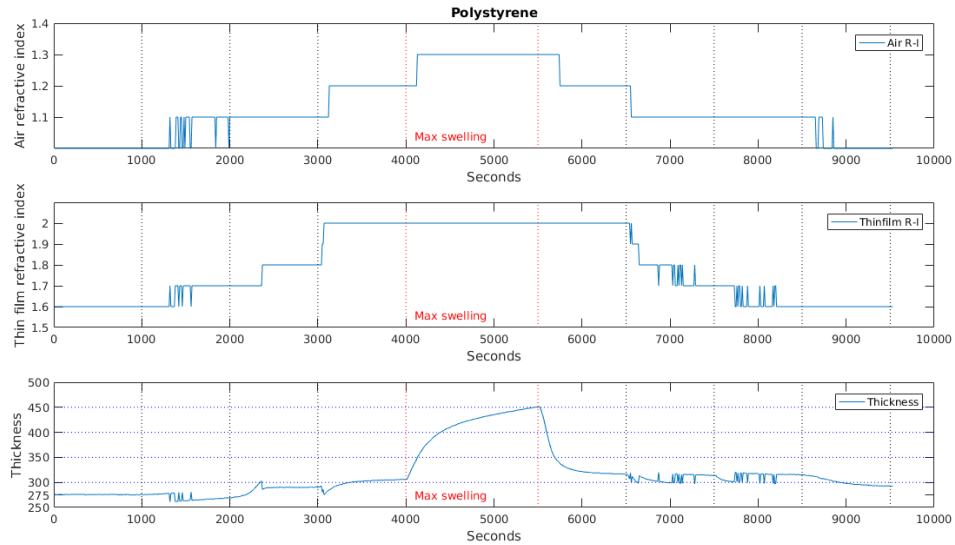


Figure 4.12: The values for the refractive index for the ambient and thin film, and the thickness has been plotted as a function of time for polystyrene. The values have been found using the fitting protocol outlined in 3.8. Vertical dotted lines have been added to represent times where the swelling protocol has increased and decreased the nitrogen gas flow and toluene vapour. The area between the red vertical dotted lines denote the maximum flow through the toluene.

increase in the mean square error after the 6500 second mark is due to the noise in the thin film refractive index. The solvent concentration in the thin film as a function of time is shown in figure 4.14.

4.5 Polyisoprene

Polyisoprene with a measured thickness of 301 nm and a refractive index 1.4594 using the single point stage, has been placed into the solvent vapour annealing chamber and swelled using the solvent vapour annealing protocol outlined in section 3.10.1. The ambient refractive index has been bounded to the interval $[1, 1.3]$ with a step size 0.1 and the thin film refractive index bounded to the interval $[1.4, 2]$ with a step size 0.1. The thin film thickness has been bounded to the interval $[250 \text{ nm}, 550 \text{ nm}]$ with a step size 1 and the silicon oxide thickness set to 2 nm. Figure 4.16 shows the values found using the fitting protocol outlined in section 3.8. The vertical dotted lines has been added to represent times where the swelling protocol has increased and decreased the nitrogen gas flow and toluene vapour. Horizontal lines have been added to the thickness plot to help the reader. The thickness of

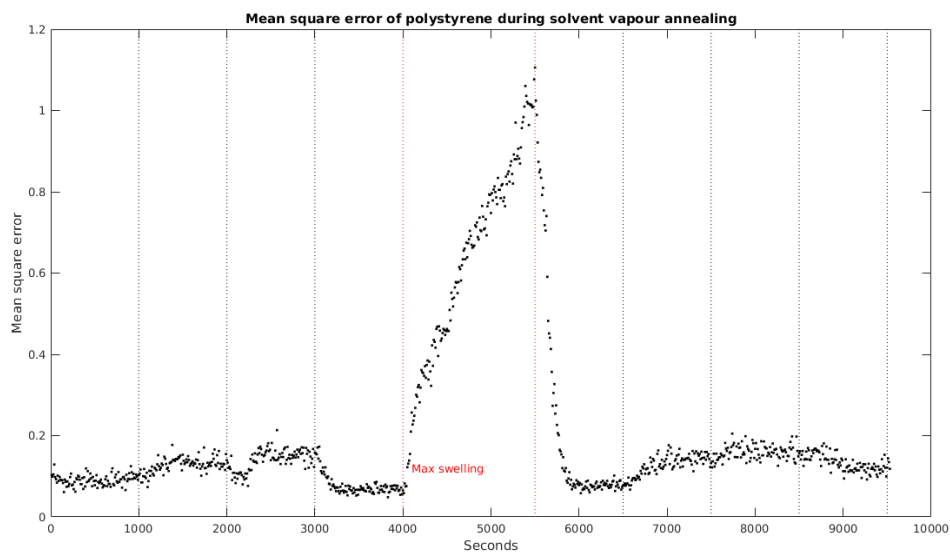


Figure 4.13: The mean square error has been plotted as a function of time. The mean square error can be seen to increase at the 1500 and 2500 mark due to the noise in the modelling and drop in thickness values. The mean square error increases from 0.1 to 1 during the max toluene swelling, this is due to the reflectance measurements decreasing in value during this time and creating a gap between the fresnel reflectance equation and reflectance. The increase in the mean square error after the 6500 second mark is due to the noise in the thin film refractive index.

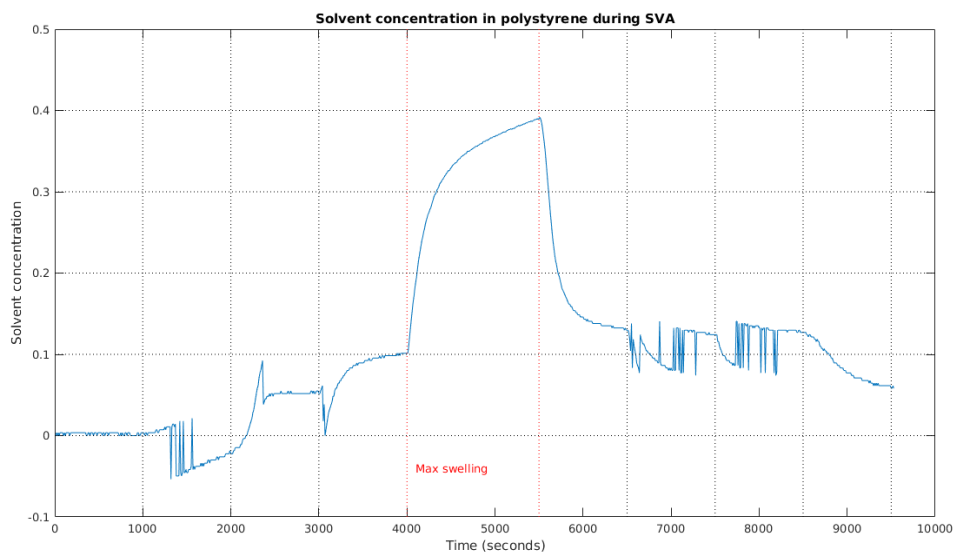


Figure 4.14: The solvent concentration in the polystyrene as a function of time.

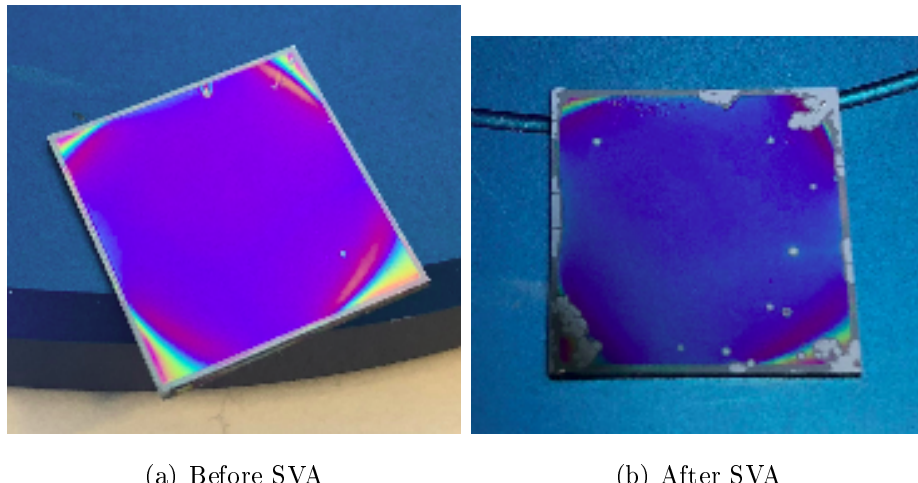


Figure 4.15: Before and after solvent vapour annealing photos of polystyrene

the polyisoprene shows a slow uptake of the toluene vapour during the first 4000 seconds. The thickness of polyisoprene increases from 300 nm to 400 nm. During this time the polyisoprene refractive index increases from [1.4] to [1.6]. The jumps in the polyisoprene refractive index at the 2000 and 3000 mark coincide with little spikes in the thickness values. The ambient refractive index at the 3000 second mark is erratic, and further along around the 3500 second mark the ambient refractive index drops back to 1. During the maximum swelling of the polyisoprene, the refractive indices and thickness increase. There are dips in the thickness during the maximum swelling which coincide with the increase of the polyisoprene refractive index, 1.6 to 1.7 and 1.7 to 1.8, and increase of the ambient refractive index, 1.2 to 1.3. Deswelling starts at the 5500 second mark and the thickness drops from 550 nm to 400 nm with in 1000 seconds. The thickness measurements continue to decrease and the drops in thickness coincide with the decrease in polyisoprene refractive index. The mean square error increases around the 2000 second mark when the ambient refractive index and the polyisoprene refractive index increase. The mean square error increases during the maximum swelling interval from 0.1 to 0.8. During the maximum swelling there are three mini increases in the mean square error, the first increase coincides with the increase of the ambient refractive index from 1.1 to 1.2. The second coincides with the increase of both the ambient and polyisoprene refractive index, from 1.2 to 1.3 and 1.6 to 1.7 respectively. The third coincides with the increase of the polyisoprene refractive index from 1.7 to 1.8. The mean square error variation after the maximum swelling coincide with the decreases polyisoprene refractive index. The solvent concentration in the thin film as a function of time is shown in figure 4.18.

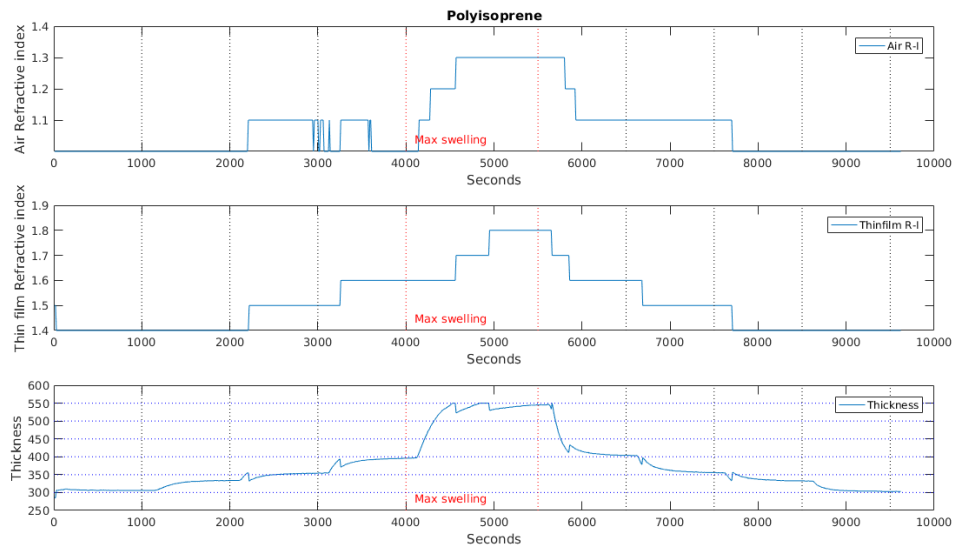


Figure 4.16: The values for the refractive index for the ambient and thin film, and the thickness has been plotted as a function of time for polyisoprene. The values have been found using the fitting protocol outlined in 3.8. Vertical dotted lines have been added to represent times where the swelling protocol has increased and decreased the nitrogen gas flow and toluene vapour. The area between the red vertical dotted lines denote the maximum flow through the toluene.

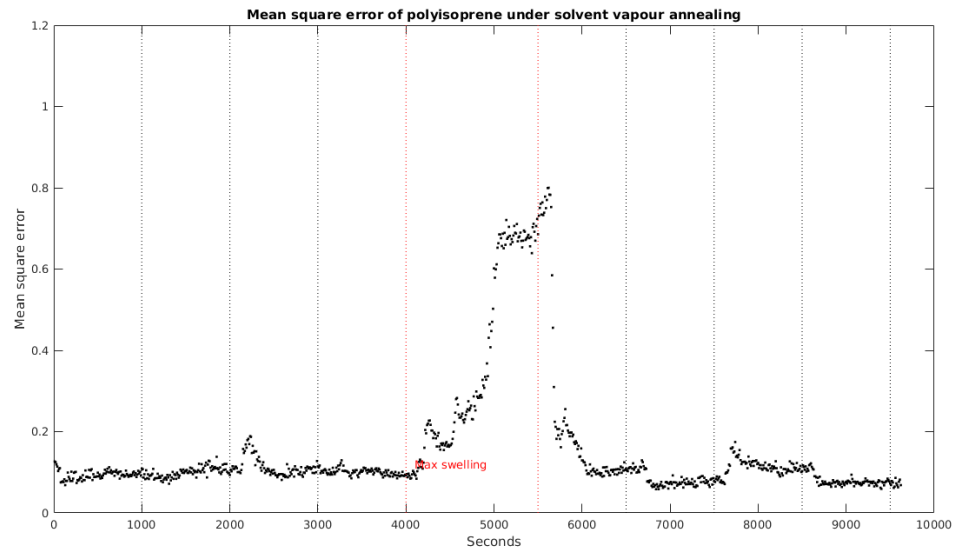


Figure 4.17: The mean square error has been plotted as a function of time.

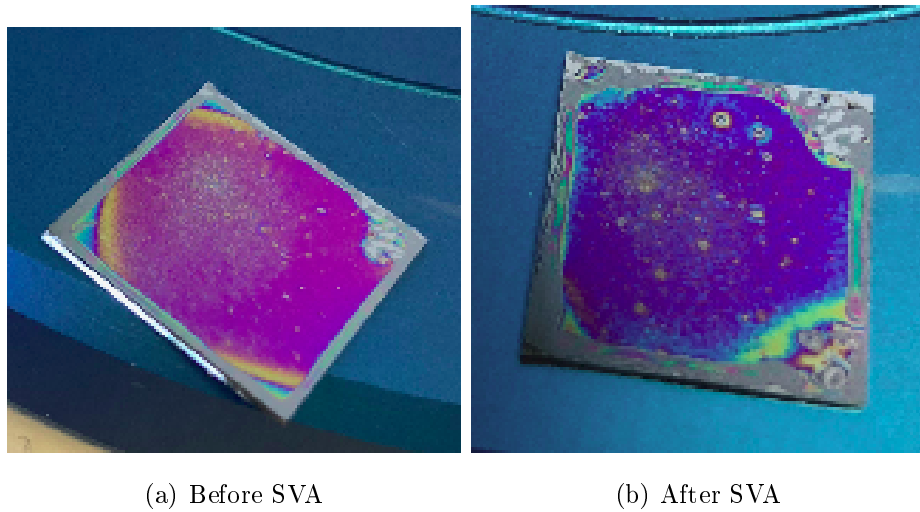


Figure 4.19: Before and after solvent vapour annealing photos of polyisoprene

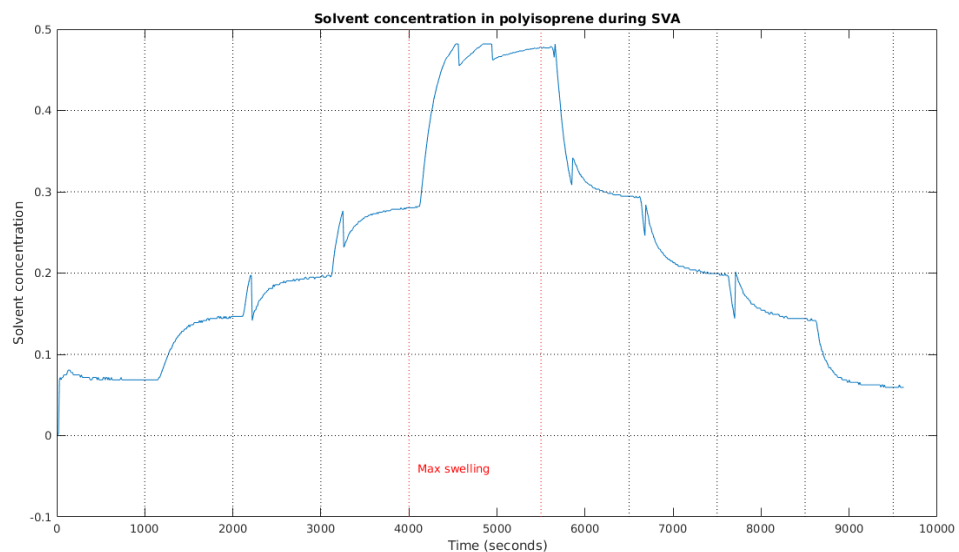


Figure 4.18:

4.6 Polystyrene-*b*-polyisoprene

Chapter 5

Bibliography

- [1] Jianqi Zhang, Dorthe Posselt, Detlef-M. Smilgies, Jan Perlich, Konstantinos Kyriakos, Sebastian Jaksch, and Christine M. Papadakis. Lamellar diblock copolymer thin films during solvent vapor annealing studied by gisaxs: Different behavior of parallel and perpendicular lamellae. *Macromolecules*, 47(16):5711–5718, 2014. PMID: 25197146.
- [2] I. Levine. *Physical Chemistry*. McGraw-Hill, 1995.
- [3] H. Fujiwara. *Spectroscopic Ellipsometry: Principles and Applications*. Wiley, 2007.
- [4] H.G. Tompkins and J.N. Hilfiker. *Spectroscopic Ellipsometry: Practical Application to Thin Film Characterization*. Materials Characterization and Analysis Collection. Momentum Press, 2015.
- [5] R.A.L. Jones. *Soft Condensed Matter*. Oxford Master Series in Physics. OUP Oxford, 2002.
- [6] G.R. Strobl. *The Physics of Polymers: Concepts for Understanding Their Structures and Behavior*. Springer Berlin Heidelberg, 2007.
- [7] Frank S. Bates and Glenn Fredrickson. Block copolymer thermodynamics: Theory and experiment. *Annual review of physical chemistry*, 41:525–57, 10 1990.
- [8] Daniel J. Kozuch, Wenlin Zhang, and Scott T. Milner. Predicting the flory-huggins parameter for polymers with stiffness mismatch from molecular dynamics simulations. *Polymers*, 8(6), 2016.
- [9] M.C. Petty. *Molecular Electronics: From Principles to Practice*. Wiley Series in Materials for Electronic & Optoelectronic Applications. Wiley, 2008.

- [10] Christophe Sinturel, Marylène Vayer, Michael Morris, and Marc A. Hillmyer. Solvent vapor annealing of block polymer thin films. *Macromolecules*, 46(14):5399–5415, 2013.
- [11] Dorthe Posselt, Jianqi Zhang, Detlef-M. Smilgies, Anatoly V. Berezkin, Igor I. Potemkin, and Christine M. Papadakis. Restructuring in block copolymer thin films: In situ gisaxs investigations during solvent vapor annealing. *Progress in Polymer Science*, 66:80–115, 2017.
- [12] Ocean Optics. *NanoCalc Software Manual*, version 4 edition, 2014.
- [13] Bronkhorst. *El-Flow® select Brochure*. Available at <https://www.bronkhorst.com/products/gas-flow/el-flow-select/f-201cv/>.
- [14] A. Baruth, Myungeun Seo, Chun Hao Lin, Kern Walster, Arjun Shankar, Marc A. Hillmyer, and C. Leighton. Optimization of long-range order in solvent vapor annealed poly(styrene)-block-poly(lactide) thin films for nanolithography. *ACS Applied Materials & Interfaces*, 6(16):13770–13781, 2014. PMID: 25029410.

Appendix A

Fresnel functions and Dispersion files

A.1 Functions

```
1 function [r_jk] = fresnel_am_s(n_j,n_k)
2
3 r_jk = (n_k-n_j)./(n_k+n_j);
4
5 end
```

```
1 function [beta] = filmpphasethickness(lamda,n_k,d_k)
2
3 beta = (2.*pi.*d_k.*n_k)./(lamda);
4
5 end
```

```
1 function [r_jkl] = fresnel_am_tf_s(n_j,n_k,n_l,d_k,lambda)
2
3 r_jkl = (fresnel_am_s(n_j,n_k)+fresnel_am_s(n_k,n_l) ...
4     .*exp(-2i.*filmpphasethickness(lambda,n_k,d_k)))./ ...
5     (1+fresnel_am_s(n_j,n_k).*fresnel_am_s(n_k,n_l) ...
6     .*exp(-2.*1i.*filmpphasethickness(lambda,n_k,d_k)));
7
8 end
```

```
1 function [r_jklm] = fresnel_am_tf_lay_sub(n_j,n_k,n_l,n_m,d_k,d_l,lambda)
2
3 r_jklm = (fresnel_am_s(n_j,n_k)+ fresnel_am_tf_s(n_k,n_l,n_m,d_l,lambda).* ...
4     exp(-2i.*filmpphasethickness(lambda,n_k,d_k))). ...
5     ./ (1+fresnel_am_s(n_j,n_k).*fresnel_am_tf_s(n_k,n_l,n_m,d_l,lambda).* ...
6     exp(-2i.*filmpphasethickness(lambda,n_k,d_k)));
7
8 end
```

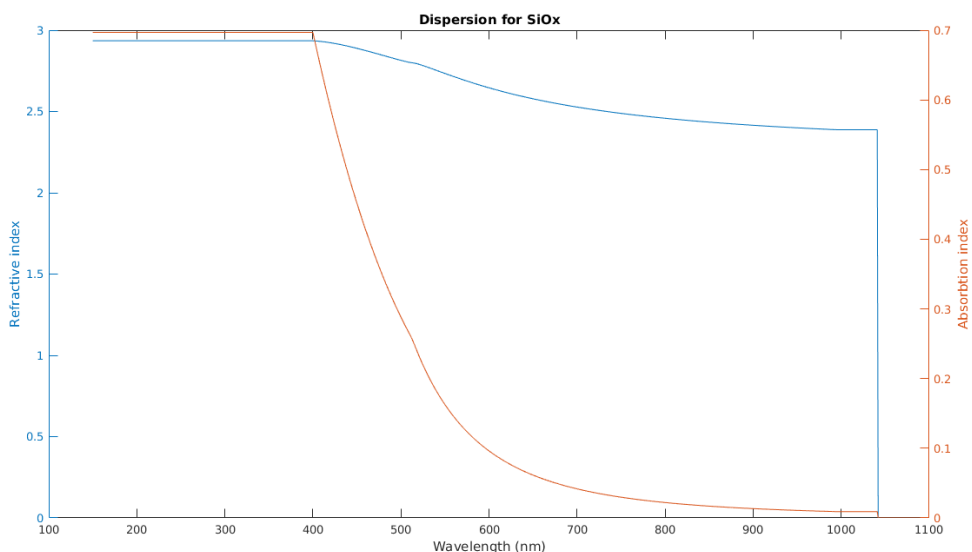
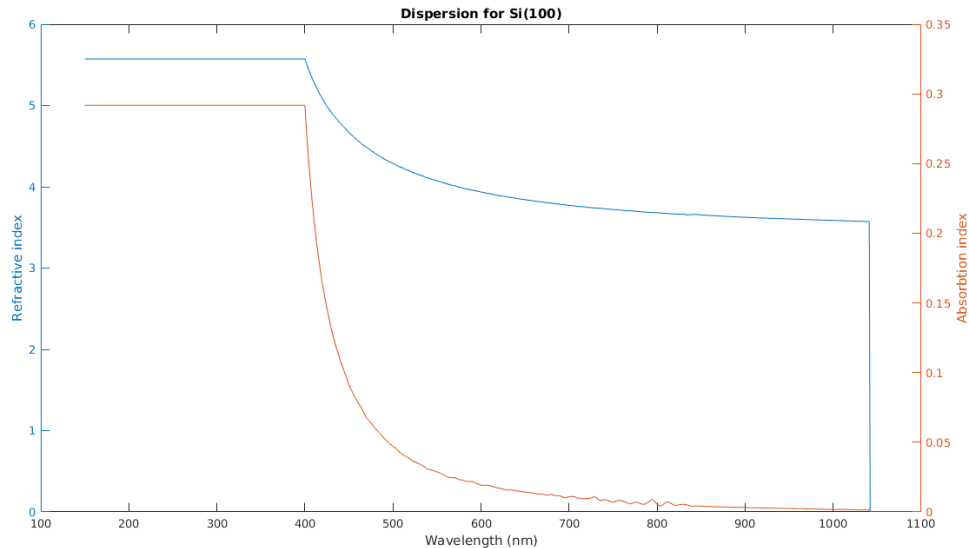
```
1 function n_c = cauchy(lambda,A,B,C)
2
```

```

3 n_c = A + (B./(lamda.^2)) + (C./(lamda.^4));
4
5 end

```

A.2 Dispersion files curves



```

1 clear all
2 close all
3
4 %% Dispersion files curves
5 % Dispersions %
6 %% Dispersion files curves

```

```
7
8 load dispersion_Si(100).dat
9 wl = dispersion_Si_100(:,1);
10 x = dispersion_Si_100(:,2);
11 y = dispersion_Si_100(:,3);
12
13 load dispersion_SiOx.dat
14 wl2 = dispersion_SiOx(:,1);
15 x2 = dispersion_SiOx(:,2);
16 y2 = dispersion_SiOx(:,3);
17
18 %%%%%%
19 % Plotting %
20 %%%%%%
21
22 figure
23 yyaxis left
24 plot(wl,x)
25 title('Dispersion for Si(100)')
26 xlabel('Wavelength (nm)')
27 ylabel('Refractive index')
28 xlim([100 1100])
29
30 yyaxis right
31 plot(wl,y)
32 ylabel('Absorbtion index')
33
34
35 figure
36 yyaxis left
37 plot(wl2,x2)
38 title('Dispersion for SiOx')
39 xlabel('Wavelength (nm)')
40 ylabel('Refractive index')
41 xlim([100 1100])
42
43 yyaxis right
44 plot(wl2,y2)
45 ylabel('Absorbtion index')
```

Appendix B

Scripts

B.1 SVA Protocol - slowslow.fps

```
1 [Generator]
2 Application=FlowPlot
3 Version=V3.34
4 [Script]
5 Repeat=1
6 SendSetpointAfter=false
7 001="1.0;    0.0;  2;  9"
8 002="1.0;    0.0;  3;  9"
9 003="1.0;    0.0;  1;  9"
10 004="1000.0;   50.0;  1;  9"
11 005="1.0;    37.5;  1;  9"
12 006="1000.0;   25.0;  2;  9"
13 007="1.0;    25.0;  1;  9"
14 008="1000.0;   50.0;  2;  9"
15 009="1.0;    12.5;  1;  9"
16 010="1000.0;   75.0;  2;  9"
17 011="1.0;    0.0;  1;  9"
18 012="1500.0;   100.0; 2;  9"
19 013="1.0;    12.5;  1;  9"
20 014="1000.0;   75.0;  2;  9"
21 015="1.0;    25.0;  1;  9"
22 016="1000.0;   50.0;  2;  9"
23 017="1.0;    37.5;  1;  9"
24 018="1000.0;   25.0;  2;  9"
25 019="1.0;    50.0;  1;  9"
26 020="1000.0;   0.0;  2;  9"
```

B.2 Light Source fluctuation study

```
1 clear all
2 close all
```

```

3
4 %%%%%%
5 % Load data %
6 %%%%%%
7
8 load daystudyreflectance
9 y = transpose(daystudyreflectance);
10 arraylength = length(daystudyreflectance(:,1)) ;
11
12 %%%%%%
13 % Physics %
14 %%%%%%
15
16 wavelength = [400:1041];
17
18 %%%%%%
19 % Plotting %
20 %%%%%%
21
22 hold on
23
24 for q = 1: arraylength
25
26
27 plot(wavelength,y(:,q))
28 title('Light Source fluctuation study at different times of the day')
29 xlabel('Wavelength (nm)')
30 ylabel('Reflectance')
31 legend('10.47','11.19','11.49','12.19','12.49',
32 '13.19','13.49','14.19','14.49','15.19','15.49','16.19','16.49','17.19')
33 axis([400 1041 0 1])
34
35 end
36
37 hold off

```

B.3 Nano-Calc simulated reflectance curve

```

1 clear all
2 close all
3
4
5 %%%%%%
6 % Air_SI(100)_Air.xy %
7 %%%%%%
8
9 %%%%%%
10 % Load data %
11 %%%%%%
12
13 load Air_SI(100)_Air.xy

```

```

14
15 x = Air_SI_100_Air(:,1);
16 y = Air_SI_100_Air(:,2);
17
18
19 %%%%%%
20 % Physics %
21 %%%%%%
22
23 wavelength = [400:1041];
24
25 %%%%%%
26 % Refractive index %
27 %%%%%%
28
29 n_0 = 1;
30
31 load dispersion_Si(100).dat
32 disp = dispersion_Si_100_(251:1:892,:);
33 n_1 = transpose(disp(:,2))-1i.*transpose(disp(:,3));
34
35
36
37 %%%%%%
38 % Calculations %
39 %%%%%%
40
41 r_01 = fresnel_am_s(n_0,n_1)
42
43 R_01 = r_01.*conj(r_01);
44
45 plot(x,y,'g',wavelength,R_01,'--k')
46 title({'Fresnel reflectance equation plotted on NanoCalc simulated reflectance ...',
        'curve'})]
47 xlabel('Wavelength(nm)')
48 ylabel('Reflectance(%)')
49 legend('Simulation','Fresnel')
```

```

1 clear all
2 close all
3
4
5 %%%%%%
6 % Air_n1_5_SI(100)_Air.xy %
7 %%%%%%
8
9 %%%%%%
10 % Load data %
11 %%%%%%
12
13 load Air_n1_5_SI(100)_Air.xy
14
15 x = Air_n1_5_SI_100_Air(:,1);
```

```

16 y = Air_n1_5_SI_100_Air(:,2);
17
18
19 %%%%%%
20 % Physics %
21 %%%%%%
22
23 wavelength = [400:1041];
24
25 %%%%%%
26 % Refractive index %
27 %%%%%%
28
29 n_0 = 1;
30 n_1 = 1.5;
31
32 load dispersion_Si(100).dat
33 disp = dispersion_Si_100_(251:1:892,:);
34 n_2 = transpose(disp(:,2))-li.*transpose(disp(:,3));
35
36 %%%%%%
37 % Thickness %
38 %%%%%%
39
40 d = 1000;
41
42
43 %%%%%%
44 % Calculations %
45 %%%%%%
46
47 r_012 = fresnel_am_tf_s(n_0,n_1,n_2,d,wavelength)
48
49 R_012 = r_012.*conj(r_012);
50
51 plot(x,y,'g',wavelength,R_012,'--k')
52 title(['Fresnel reflectance equation plotted on NanoCalc simulated reflectance ...'
         'curve'])
53 xlabel('Wavelength (nm)')
54 ylabel('Reflectance (%)')
55 legend('Simulation','Fresnel')
```

```

1 clear all
2 close all
3
4
5 %%%%%%
6 % Air_Cauchy_SiOx_SI(100).xy %
7 %%%%%%
8
9 %%%%%%
10 % Load data %
11 %%%%%%
```

```

12
13 load Air_Cauchy_SiOx(2nm)_SI.xy
14
15 x = Air_Cauchy_SiOx_2nm_SI(:,1);
16 y = Air_Cauchy_SiOx_2nm_SI(:,2);
17
18
19 %%%%%%
20 % Physics %
21 %%%%%%
22
23 wavelength = [400:1041];
24
25 %%%%%%
26 % Refractive index %
27 %%%%%%
28
29 n_0 = 1;
30
31 A = 1.4450;
32 B = 3e4;
33 C = 4e7;
34 n_1 = cauchy(wavelength,A,B,C);
35
36 load dispersion_SiOx.dat
37 disp1 = dispersion_SiOx(251:1:892,:);
38 n_2 = transpose(disp1(:,2))-li.*transpose(disp1(:,3));
39
40 load dispersion_Si(100).dat
41 disp2 = dispersion_Si_100_(251:1:892,:);
42 n_3 = transpose(disp2(:,2))-li.*transpose(disp2(:,3));
43
44 %%%%%%
45 % Thickness %
46 %%%%%%
47
48 d1 = 1000;
49 d2 = 2;
50
51 %%%%%%
52 % Calculations %
53 %%%%%%
54
55 r_0123 = fresnel_am_tf_lay_sub(n_0,n_1,n_2,n_3,d1,d2,wavelength);
56
57 R_0123 = r_0123.*conj(r_0123);
58
59 plot(x,y,'g',wavelength,R_0123,'--k')
60 title({'Fresnel reflectance equation plotted on NanoCalc simulated reflectance ...',
       'curve'})]
61 xlabel('Wavelength(nm)')
62 ylabel('Reflectance(%)')
63 legend('Simulation','Fresnel')
```

B.4 Solvent vapour annealing ambient study

```

1 clear all
2 close all
3
4 tic
5
6 %%%%%%
7 % Physics %
8 %%%%%%
9
10 wavelength = (450:900);
11
12 air = [1:0.1:2]; %Defining Refractive index limits.
13
14 framevalues = []; %Define empty array where all data will be saved.
15
16 %%%%%%
17 % Load data %
18 %%%%%%
19
20 load ambientinvestreflectance
21
22
23 %%%%%%
24 % Loop %
25 %%%%%%
26
27 it = length(ambientinvestreflectance(:,1));
28
29 % For loop for fitting each SVA measurement.
30 for z = 1:it
31
32 y = ambientinvestreflectance(z,:);
33
34 MSE = []; %Define empty array to save data for one full SVA Measurement.
35
36 %%%%%%
37 % Reflective Index %
38 %%%%%%
39
40
41 % For loop for fitting refractive index of Air.
42 for k = 1:length(air)
43
44 list = [];
45
46 n_0 = air(k);
47
48
49
50
51 load dispersion_SiOx.dat

```

```

52     disp_2 = dispersion_SiOx(301:1:751,:);
53     n_1 = transpose(disp_2(:,2)) -li.*transpose(disp_2(:,3));
54
55     load dispersion_Si(100).dat
56     disp_3 = dispersion_Si_100_(301:1:751,:);
57     n_2 = transpose(disp_3(:,2)) -li.*transpose(disp_3(:,3));
58
59
60 %%%%%%%%%%%%%%
61 % Thickness %
62 %%%%%%%%%%%%%%
63
64     d_1 = 2;
65
66 %%%%%%%%%%%%%%
67 % Reflectance Calculations %
68 %%%%%%%%%%%%%%
69
70     r_01 = fresnel_am_tf_s(n_0,n_1,n_2,d_1,wavelength);
71
72     R_01 = r_01.*conj(r_01);
73
74
75 %%%%%%
76 % MSE %
77 %%%%%%
78
79     Δy = y - R_01;
80     sqΔy = Δy.^2;
81     sumsq = sum(sqΔy)./length(wavelength);
82
83
84     list = [air(k),sumsq];
85     MSE = vertcat(MSE,list);
86
87     end
88
89 [row,column] = find(MSE==min(min(MSE(:,2))));
90 tempvalue = MSE(row,:);
91
92 framevalues = vertcat(framevalues,tempvalue);
93
94 end
95
96 %save('frame_val.mat','framevalues') %Saving to file
97
98 toc

```

```

1 clear all
2 close all
3
4 %%%%%%
5 % Load Data %

```

```

6 %%%%%%
7
8 load ambientinvestreflectance
9 load frame_val.mat
10
11 %%%%%%
12 % Physics %
13 %%%%%%
14
15 wavelength = (450:900);
16
17 %%%%%%
18 % Plotting %
19 %%%%%%
20
21 figure('units','normalized','outerposition',[0 0 1 1])
22 plot((12:length(ambientinvestreflectance(:,1))).*10,
23 framevalues(12:length(ambientinvestreflectance(:,1)),1))
24 axis([0 11000 1 1.4])
25 title('Solvent vapour annealing ambient study')
26 xlabel('Seconds')
27 ylabel('Refractive Index')
28 yticks([1 1.1 1.2 1.3 ])
29 legend('Refractive index of Ambient')
30 hold on
31 line1 = vline([1000 2000 3000 4000 5500 6500 7500 8500 ...
    9500],{'k:','k:','k:','r:','r:','k:','k:'},{'','','','Max ...
    swelling','','','',''});
32 hold off
33
34
35 figure('units','normalized','outerposition',[0 0 1 1])
36 plot((12:length(ambientinvestreflectance(:,1))).*10,
37 framevalues(12:length(ambientinvestreflectance(:,1)),2).*length(wavelength), 'k.')
38 axis([0 11000 0 0.3])
39 title('Solvent vapour annealing ambient study - MSE')
40 xlabel('Seconds')
41 ylabel('MSE')
42 hold on
43 line1 = vline([1000 2000 3000 4000 5500 6500 7500 8500 ...
    9500],{'k:','k:','k:','r:','r:','k:','k:'},{'','','','Max ...
    swelling','','','',''});
44 hold off

```